

QUANTIFYING THE ENERGETICS OF BINDING BETWEEN p53 AND DNA
USING ELECTROPHORETIC MOBILITY SHIFT ASSAYS

THESIS

Presented to the Graduate Council of
Texas State University – San Marcos
in Partial Fulfillment
of the Requirements

for the Degree

Master of SCIENCE

by

Leasha J. Schaub, B.S.

San Marcos, Texas
December 2012

QUANTIFYING THE ENERGETICS OF BINDING BETWEEN p53 AND DNA
USING ELECTROPHORETIC MOBILITY SHIFT ASSAYS

Committee Members Approved:

Steven Whitten, Chair

Rachell Booth

Kevin Lewis

Approved:

J. Michael Willoughby
Dean of the Graduate College

Copyright

by

Leasha Janece Schaub

2012

FAIR USE AND AUTHOR'S PERMISSION STATEMENT

Fair Use

This work is protected by the Copyright Laws of the United States (Public Law 94-553, section 107). Consistent with fair use as defined in the Copyright Laws, brief quotations from this material are allowed with proper acknowledgement. Use of this material for financial gain without the author's express written permission is not allowed.

Duplication Permission

As the copyright holder of this work, I, Leasha Janece Schaub, refuse permission to copy in excess of the "Fair Use" exemption without my written permission.

TO MY FATHER AND MOTHER

ACKNOWLEDGEMENTS

First and foremost, I would like to thank my advisor, Dr. Steven Whitten, for all of his encouragement and guidance. To whom without, this thesis would not have been successfully completed. While working underneath him, I have not only broaden my knowledge and critical thinking but as a person, as well. I would also like to thank my committee members, Dr. Rachell Booth and Dr. Kevin Lewis, for their support and patience while critically reviewing this thesis. A special thanks goes to Dr. Ron Walter for allowing the use of his laboratory equipment, without, this project would not have succeed.

To my fellow Whitten group researchers, graduates and undergraduates, thank you for making lab enjoyable and allowing there to never be a dull moment. Without their support and sarcasm, I would not have made it through these past two years. I especially would like to thank, my fellow p53 graduate student, Jessica Tracy, who has been beside me every step of the way.

Lastly, to my family, who have always pushed me to strive for my goals and have never lost faith in me. An extremely special thank you goes to my parents, Lowry and Janice Schaub, for supporting me in more than one way, through out my graduate and undergraduate career.

This manuscript was submitted on August 31, 2012.

TABLE OF CONTENTS

	Page
ACKNOWLEDGEMENTS.....	vi
LIST OF TABLES.....	ix
LIST OF FIGURES.....	x
ABSTRACT.....	xii
 CHAPTER	
I. INTRODUCTION.....	1
II. MATERIALS AND METHODS.....	7
2.1 Materials.....	7
2.2 Cloning, Over-Expression, and Purification of Recombinant Human p53.....	7
2.2.1 Cloning and transformation.....	7
2.2.2 Glycerol stocks.....	9
2.2.3 Bacterial over-expression.....	10
2.2.4 Purification from cell lysate.....	11
2.2.5 Thrombin digestion.....	13
2.3 Protein Detection Methods.....	13
2.3.1 SDS-PAGE to judge sample purity.....	13
2.3.2 SDS-PAGE to judge protein concentration.....	16
2.3.3 Western blot detection of p53.....	19
2.3.4 Glutaraldehyde cross-linking to detect oligomerization.....	21
2.4 DNA Synthesis and Sample Preparation.....	23

2.4.1 DNA synthesis	23
2.4.2 Spectroscopic determination of ssDNA concentration	26
2.4.3 Preparation of DNA oligomers	29
2.4.4 Spectroscopic determination of dsDNA concentration.....	30
2.5 Detection of p53:DNA Binding	32
2.5.1 EMSA using dsDNA with SYBR-gold.....	32
2.5.2 EMSA using dsDNA with FAM-label	34
2.6 Gel Imaging and Analysis.....	34
2.6.1 Imaging of coomassie stained protein gels and western blots	34
2.6.2 Imaging of SYBR-gold stained DNA.....	36
2.6.3 Imaging of FAM-labeled DNA.....	36
2.6.4 Analysis of gel images for protein concentration	37
2.6.5 Analysis of gel images for protein:DNA binding.....	37
III. RESULTS AND DISCUSSION	39
3.1 Purification of Recombinant p53 and Thrombin Cleavage	39
3.2 Determination of p53 Oligomerization.....	39
3.3 Determination of p53 Energetic Binding Constant	45
IV. CONCLUSIONS.....	57
REFERENCES	60

LIST OF TABLES

Table	Page
2.1 The Nearest Neighbor Extinction Coefficients ($\text{L mol}^{-1} \text{ cm}^{-1}$) for the Neighboring Nucleotides i and $i + 1$	27
2.2 Individual Extinction Coefficient ($\text{L mol}^{-1} \text{ cm}^{-1}$) for Individual Nucleotides i	28
3.1 Binding Kinetics Determined through EMSA for WTp53 and Hp53	55

LIST OF FIGURES

Figure	Page
1.1 Schematic of p53's Two Regulatory Pathways	2
1.2 Diagram Representation of p53 Domains	3
2.1 Wild Type and Hyperstable p53 Amino Acid Sequences (1-363)	8
2.2 His-Tagged p53 Purification Elution Profile Schematic.....	12
2.3 SDS-PAGE of 6x-Histidine Tag Thrombin Cleavage.....	14
2.4 SDS-PAGE of p53 Purification Steps.....	17
2.5 p53 Concentration Determination by SDS-PAGE.....	20
2.6 Detection of p53 through Western Blot Analysis	22
2.7 Visualization of p53 Oligomerization State by Glutaraldehyde Cross-Linking	24
2.8 Single-Stranded DNA (ssDNA) Sequences.....	25
2.9 Visualization of dsDNA Oligomerization.....	31
2.10 Double-Stranded DNA (dsDNA) Sequences.....	33
2.11 Example of EMSA Using FAM-Labeled dsDNA.....	35
3.1 SDS-PAGE of p53 Purity After Purification	40
3.2 Oligomerization of Wild Type p53-HIS (Wtp53-his) by Glutaraldehyde Cross- Linking.....	42
3.3 Oligomerization of Wild Type p53 (Wtp53) by Glutaraldehyde Cross-Linking.....	43

3.4 Oligomerization of Hyperstable p53-HIS (Hp53-his) by Glutaraldehyde Cross-Linking.....	44
3.5 Oligomerization of Hyperstable p53 (Hp53) by Glutaraldehyde Cross-Linking.....	46
3.6 Binding Kinetics of Non-Labeled dsDNA Control for Recognition Sequences p21 and PG by EMSA	48
3.7 Binding Kinetics of Thrombin Control for Recognition Sequences p21 and PG by EMSA	50
3.8 Binding Kinetics of Wild Type p53-HIS for Recognition Sequences p21 and PG by EMSA	51
3.9 Binding Kinetics of Wild Type p53 for Recognition Sequences p21 and PG by EMSA	52
3.10 Binding Kinetics of Hyperstable p53-His for Recognition Sequences p21 and PG by EMSA	53
3.11 Binding Kinetics of Hyperstable p53 for Recognition Sequences p21 and PG by EMSA	54

ABSTRACT

QUANTIFYING THE ENERGETICS OF BINDING BETWEEN P53 AND DNA USING ELECTROPHORETIC MOBILITY SHIFT ASSAYS

by

Leasha Janece Schaub, B.S.

Texas State University-San Marcos

December 2012

SUPERVISING PROFESSOR: STEVEN WHITTEN

A new class of proteins has been termed “intrinsically disordered” or “ID” for short. The proteins within this class appear to lack tertiary stability, though protein structure has been linked to function in the past. These ID proteins are also prevalent, especially in eukaryotic proteins (~30%) and transcriptional factors (~70%). The high occurrence of ID suggest that this natively unfolded motif has been evolutionary selected. One of these ID proteins is the tumor suppressor protein p53. The p53 protein is a transcription factor that plays a role in ensuring genomic integrity. p53 is a homotetramer made up of seven domains with only two of the seven domains being natively folded. The other five domains lack tertiary structure under physiological conditions. It has been seen

that these ID domains play a role in p53 regulation, suggesting allosteric communication. p53 is highly studied due to its connection with cancer. In approximately 50% of human tumor cells there is a mutation within the p53 gene, leading to p53 to be highly studied. Because of p53's connection with cancer a database showing the frequency of mutations that effect p53 function is already available, making p53 a plausible model for how the ID motif plays a role in regulatory mechanisms. To under stand how p53 transduces signals a mutational screen on binding energetics will be done.

Before this bigger project and to show practicality of its success, basic protocols need to be established. The main focus of this thesis is exactly that. In this body of work its shown that wild type p53 and hyperstable p53 can be expressed and purified and used in binding studies. While the wild type p53 seems to be unpredictable due to its ability to form tetramers, the hyperstable p53 shows promising results for continuation with the mutational screen.

CHAPTER I

INTRODUCTION

The p53 protein, also known as the tumor suppressor protein, is a conserved transcriptional factor found in all multicellular organisms, and whose regulatory function is to ensure genomic integrity.¹⁻³ When DNA damage is sensed by the cell, cofactors activate p53 transactivating genes for one of the two pathways⁴ shown in Figure 1.1: a) initiates cellular growth arrest, and recruits other transcriptional machinery to correct the DNA damage or b) if the DNA is beyond repair, initiate apoptosis. Cancer and p53 have been linked because in the presence of non-functional p53, damaged cellular DNA proliferates, causing the formation of tumors. Approximately 50% of tumor cell lines contain missense mutations in the p53 gene causing a decrease in p53 activity.⁵⁻⁶ It has been seen that upon the introduction of functionally active p53, tumor regression occurs, making p53 one of the main targets for cancer therapeutics.⁷⁻⁹

Structurally, p53 is a 393 amino acid protein containing seven distinct domains: Activation Domain 1 (AD1), Activation Domain 2 (AD2), Proline Rich Domain (PRD), DNA Binding Domain (DBD), Nuclear Localization Signal (NLS), Tetramerization Domain (TD) and Basic Domain (BD). The ordering of these different domains is shown in Figure 1.2. Each domain carries out different roles in relation to p53 function: AD1

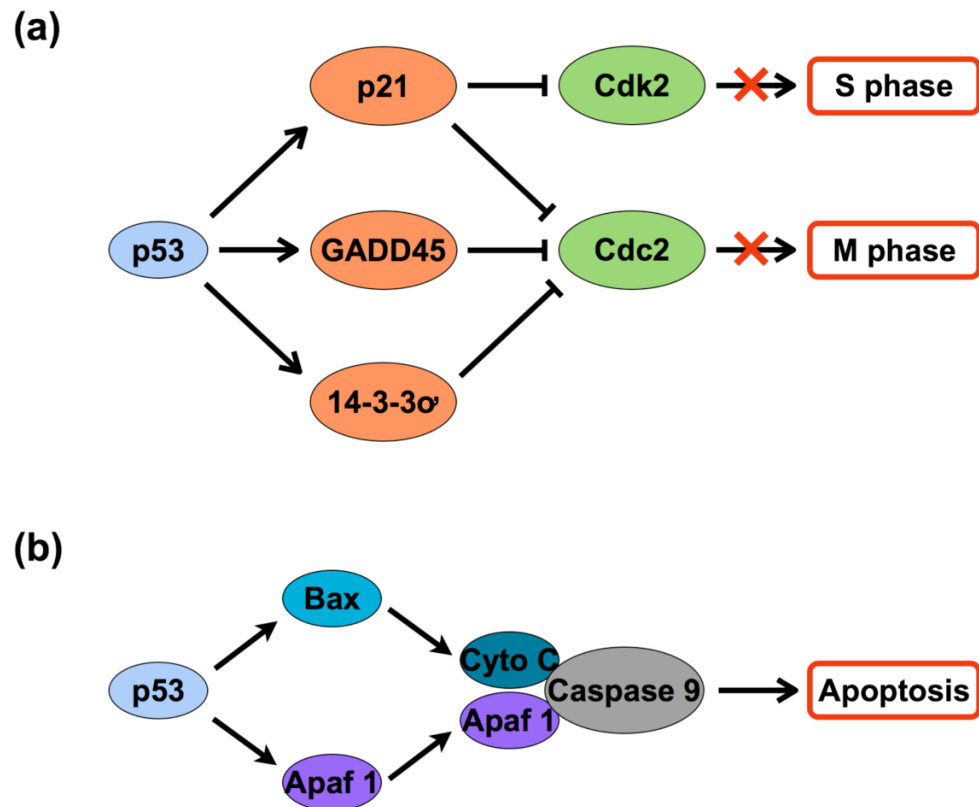


Figure 1.1. Schematic of p53's Two Regulatory Pathways. (a) A diagram showing the different interactions that can occur in p53's cellular growth arrest pathway. (b) A diagram showing a p53 pathway for apoptosis.

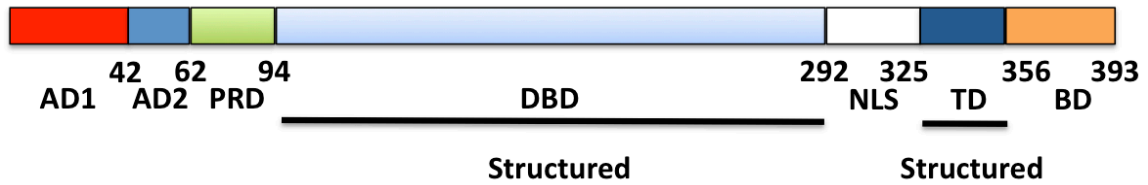


Figure 1.2. Diagram Representation of p53 Domains. Above is a schematic layout of the seven domains in a p53 monomer. The only two domains that are natively folded under physiological conditions are the DNA Binding Domain (DBD) and the Tetramerization Domain (TD). The other five are unfolded under physiological conditions and considered intrinsically disordered (ID). These consist of the Activation Domain 1 (AD1), Activation Domain 2 (AD2), Proline Rich Domain (PRD), Nuclear Localization Signal (NLS) and the Basic Domain (BD).

and AD2 are activation domains, PRD and BD are negative regulatory domains, DBD binds recognition sequences, TD forms tetramers, and the NLS directs p53 to the nucleus.

The p53 protein has also been included in a new class of proteins that are referred to as “intrinsically disordered”.¹⁰⁻¹² These proteins appear to lack tertiary stability¹³⁻¹⁵, which is surprising considering the complimentary relationships between protein structure and biological function¹⁶⁻¹⁸. The observation that intrinsically disordered (ID) proteins are common¹³⁻¹⁵, biologically active¹⁰, and often have regulatory roles mediating signaling pathways¹⁹ thus was not expected. Most transcriptional factors are thought to be ID¹⁹, and p53 like wise contains large domains that lack tertiary structure under physiological conditions²⁰⁻²². These are the domains AD1, AD2, PRD, NLS, and BD, shown in Figure 1.2. Because of these domains obtaining a quaternary structure is difficult, though there are proposed structures for p53 under physiological conditions.²³ In addition, the three N-terminal ID domains of p53 are rich in proline (22 of 93 residue positions), a property that has been associated with ID¹⁹. Thus, p53 may be a good model for how the ID motif is used in regulatory processes.

Under physiological conditions, p53 forms mainly homotetramers that have latent and active states (normally inactive). The switch of p53 from latent to active occurs through multiple processes. The presence of these latent and active states suggests that p53 has allosteric properties in which perturbations distant to the DNA binding site can regulate DNA binding activity. There have been many mutations found in tumor cell lines that are within the ID domains of p53.⁵⁻⁶ Suggesting a possibility of ID domains playing a

role in the equilibrium of latent and active p53.

Activation domains, AD1 (1-42) and AD2 (43-62), play an important role in mediating interactions with cofactors, regulators, and transcriptional machinery. Though they are ID it's been seen that local folding can occur²⁴⁻²⁵; specifically in AD1 residues 18-26 form a helix upon binding to cofactors.²⁵ It's also been seen, *in vivo* and *in vitro*, that there are multiple phosphorylation sites that affect p53 activity.²⁶⁻²⁸

The PRD (63-94) contains many proline residues (12/34) and five repeats of the conserved sequence motif, PXXP (P = proline, X = any amino acid).²⁹ The PXXP motif is known to adopt a poly-L-proline II helix (PPII)³⁰, which has been seen in p53²². This PPII structure causes an extended conformation in the unfolded state³¹⁻³² and is the reason for p53's name, causing it to run to 53 kDa on an SDS-PAGE instead of its actual molecular weight, 43 kDa³³. The PRD is a negative regulatory domain and has been shown, *in vitro*, to activate p53 by deletion of the PRD^{26,34}, interaction with free PRD peptides (80-93)³⁵, or by a prolyl isomerase cis-trans-conversion (also seen *in vivo*)³⁶.

In the NLS (292-325) residues 316-325 are responsible for directing p53 to the nucleus. Though in tumor cell lines there have been mutations found outside of this area⁵⁻⁶, suggesting that the NLS may have other functions besides nuclear localization.

The BD (356-393) is a negative regulatory domain that has been extensively studied and is known to affect p53:DNA binding. There are multiple BD modifications that can activate p53:DNA binding. This can be done, *in vitro*, by the deletion of the last 30 BD residues (363-393)²⁶, interaction with free BD peptides^{35,37}, the mutation of three lysine residues (Lys-to-Ile; positions 370, 372, 373)³⁸, antibody interactions²⁶, or the

acetylation of several lysine residues (also seen *in vivo*)³⁹.

It's unknown if the functions of these ID domains are relevant only regarding cofactor interactions or if they play a role in p53's latent and active equilibrium. To better understand p53 function, and its ability to transduce signals that are important for maintaining genomic stability, we propose to investigate domain-domain communication in p53 and how structural events in one domain can influence binding activity in its DNA binding domain. Because of the strong correlation of p53 function and cancer, p53 has been studied extensively by many research groups. Surprisingly, however, no data is available in the literature that quantitatively assesses p53's ability to transduce signals between its domains. To do this, a mutagenic screen of the measured binding energetics between p53 and specific DNA recognition elements will be performed. To demonstrate feasibility in that larger project, the goal of this thesis was to: 1) express human p53 in bacterial cultures and isolate the recombinant protein from cell lysates, 2) demonstrate that recombinant p53 folds into a tetrameric structure, similar to the physiologically active species, and 3) measure the energetics of p53 binding to the *PG* and *p21* recognition elements.

CHAPTER II

MATERIALS AND METHODS

2.1 *Materials*

All chemicals and reagents that were used were Molecular Biology grade or higher. Water was filtered and deionized by a Millipore Milli-Q purification unit (Billerica, Ma). Prior to its use in sample and buffer preparation, all pipette tips and micro-centrifuge tubes were sterilized using a HICLAVE HV-50 autoclave vessel by Hirayama (Westbury, NY) prior to use. Sterile 50 mL and 15 mL conical tubes were purchased from VWR (Radnor, PA). Luria Agar plates containing 100 µg/mL ampicillin, used for growing bacterial cultures, were purchased from Teknova (Hollister, CA).

2.2 *Cloning, Over-expression, and Purification of Recombinant Human p53*

2.2.1 *Cloning and transformation*

Genes coding for residues 1-363 of human p53, wild type (WTp53) and hyperstable (Hp53), including an N-terminal 6x-histidine tag and thrombin cleavage site (MRGSHHHHHHSSGLVPRGS-p53(1-363)) were cloned into a plasmid expression vector by DNA 2.0 (Menlo Park, CA). Figure 2.1 shows the amino acid sequences used in this study, representing the consensus wild type human p53 sequence²⁶ and a

(a)

```

1  MEEPQSDPSV EPPLSQETFS DLWKLLPENN VLSPLPSQAM DDLMLSPDDI EQWFTEDPGP
61 DEAPRMPEAA PRVAPAPAAP TPAAPAPAPS WPLSSSVPSQ KTYQGSYGFR LGFLHSGTAK
121 SVTCTYSPAL NKMFCQLAKT CPVQLWVDST PPPGTRVRAM AIYKQSQHMT EVVRRCPHHE
181 RCSDSDGLAP PQHLIRVEGN LRVEYLDDRN TFRHSVVVPY EPPEVGSDCT TIHYNMCMNS
241 SCMGGMNRRP ILTIITLED SGNLLGRNSF EVRVCACPGR DRRTEENLR KKGEPPHELP
301 PGSTKRALPN NTSSSPQPKK KPLDGEYFTL QIRGRERFEM FRELNEALEL KDAQAGKEPG
361 GSR

```

(b)

```

1  MEEPQSDPSV EPPLSQETFS DLWKLLPENN VLSPLPSQAM DDLMLSPDDI EQWFTEDPGP
61 DEAPRMPEAA PRVAPAPAAP TPAAPAPAPS WPLSSSVPSQ KTYQGSYGFR LGFLHSGTAK
121 SVTCTYSPAL NKLFCQLAKT CPVQLWVDST PPPGTRVRAM AIYKQSQHMT EVVRRCPHHE
181 RCSDSDGLAP PQHLIRVEGN LRAEYLDDRN TFRHSVVVPY EPPEVGSDCT TIHYNMCMYS
241 SCMGGMNRRP ILTIITLED SGNLLGRDSF EVRVCACPGR DRRTEENLR KKGEPPHELP
301 PGSTKRALPN NTSSSPQPKK KPLDGEYFTL QIRGRERFEM FRELNEALEL KDAQAGKEPG
361 GSR

```

Figure 2.1. Wild Type and Hyperstable p53 Amino Acid Sequences (1-363). Residues 1-363 of p53 contains all domains besides the BD. The deletion of the BD is one of the many modifications that activates p53. (a) Shows the residues 1-363 for recombinant human wild type p53 (WTp53) with the BD deletion. (b) Shows the residues 1-363 for a designed quadruple mutant (M133L/V203A/N239Y/N258D) p53⁴⁰, that has improved structural stability while still having the wild types ability to bind DNA. These mutations are found in the DBD and are highlighted in red.

hyperstable variant (M133L/V203A/N239Y/N258D)⁴⁰. An algorithm developed by DNA 2.0 was used to optimize the codon usage of both Wtp53 and Hp53 genes for protein expression in *Escherichia coli* cells.⁴¹ A pJexpress bacterial vector plasmid (pJexpress404) was used that contained a T5 promoter sequence allowing for isopropyl β -D-1-thiogalactopyranoside (IPTG)-induced expression of p53 in *E. coli*.⁴² The pJexpress plasmid also contained a high-copy-number pUC origin of replication (~150-200 copies/cell), and an ampicillin resistant gene (*ampR*) allowing for selection of transformed cells, through the expression of beta-lactamase. Upon receipt from DNA 2.0, the plasmids were solubilized using DNA grade sterile water to a working concentration of 1 ng/ μ L and stored at -80°C in 10 μ L aliquots.

Transformation was done using BL21 (DE3) pLysS competent cells from Novagen (Darmstadt, Germany), where 10 μ L of plasmid stock was added to 50 μ L of 60 mM calcium chloride (CaCl₂) suspended competent cells and gently mixed. To transform cells, the sample was incubated on ice for 5 minutes, followed by a 30 second heat bath (42 °C) and 2 minute ice incubation. After transformation, 250 μ L of Super Optimal Broth with Catabolite repression (SOC) was added at room temperature, followed by aseptic dispersion of 150 μ L onto a Luria Agarose plate containing 100 μ g/mL ampicillin, allowing for transformed *E. coli* cells selection, and incubated at 37 °C for 12-24 hours.

2.2.2 Glycerol stocks

A sterile 50 mL conical tube was filled with 20 mL of sterile Luria Broth (LB) (1% (w/v) tryptone, 1% (w/v) NaCl, 0.5% (w/v) yeast extract) + 100 μ g/mL ampicillin and was aseptically inoculated with a single colony of human p53 transformed *E. coli*

cells (see section 2.2.1). Followed by incubation with orbital rotation at room temperature until turbidity was seen (~8 hours). After incubation, 800 μ L of cell culture was mixed with 200 μ L of sterile 80% glycerol and stored at -80 °C in a sterile cryovial tube.

2.2.3 *Bacterial over-expression*

For bacterial growth and protein expression, a Luria Agarose plate + 100 μ g/mL ampicillin was aseptically streaked using a glycerol stock (see section 2.2.2) and incubated at 37 °C until the appearance of colonies (12-16 hours). Due to improper refolding of p53 from the inclusion bodies, the lysate's soluble fraction was used for p53 purification. We found that growing all cell cultures at room temperature (~25 °C) helped increase expression of p53 in the soluble fraction. Upon the appearance of colonies, a sterile 50 mL conical tube containing 20 mL of sterile LB + 100 μ g/mL ampicillin was aseptically inoculated with a single colony and incubated with orbital rotation till turbidity was seen (~8 hours). The 20 mL cell culture was then transferred to 1 L of fresh sterile LB + 100 μ g/mL ampicillin and incubated with orbital rotation until reaching an OD₆₀₀ of 0.6-0.8. At this point, the 1 L cell culture was induced with 0.5 mM IPTG and incubated with orbital rotation overnight (12-16 hours). After induction, cell cultures were harvested by centrifugation, at 5,000-10,000 x g, 4 °C, for 20 minutes. The supernatant was poured off and all pellets from an 1 L prep were transferred to a sterile 50 mL conical tube and re-suspended in Storage Buffer (25 mM HEPES (pH 8), 10% (v/v) glycerol, 2 mM β -mercaptoethanol, 0.1% (v/v) Tween-20) at 2 mL/g of cells. Resuspended pellets were stored at -80 °C, and usable for one month.

2.2.4 *Purification from cell lysate*

Frozen cell pellets (see section 2.2.3) were thawed on ice for 15 minutes and suspended in 30 mL of Buffer B (0.3 M NaCl, 50 mM sodium phosphate monobasic, monohydrate (NaH₂PO₄) (pH 8.0), 20% (v/v) glycerol, 10 mM β -mercaptoethanol, 0.5 mM phenylmethylsulfonyl fluoride (PMSF), 1% (v/v) Tween-20). To weaken the cell walls, 100 μ g/mL of lysozyme was added and incubated on ice for 30 minutes. Following lysozyme incubation, cell sonication was performed using a Bronson Sonifer S-450A (Danbury, CT) at an output setting of 5 and a 60% duty cycle for 2 minutes; 10-second pulses separated by 10-second rest periods, on ice. Sonicated cells were harvested by centrifugation at 10,000 x g, 4 °C, for 10 minutes. The supernatant was saved and filtered through a Millipore 0.45 μ m syringe filter purchased from Millipore (Billerica, MA) and then mixed with ~10 mL slurry of nickel(II)-nitrilotriacetate (Ni-NTA) for purification by affinity chromatography. The N-terminal 6x-histidine tag allows for p53 to have affinity for the Ni-NTA agarose.

For purification of p53 from Ni-NTA agarose, a 10 mL bed volume of Ni-NTA resin was equilibrated with Buffer B before loading filtered supernatant. The column was washed with 30-40 mL of Buffer B to elute flowthrough (FT), followed by 25 mL of Buffer C (0.3 M NaCl, 50 mM NaH₂PO₄ (pH 8.0), 20% (v/v) glycerol, 10 mM β -mercaptoethanol, 0.5 mM PMSF, 40 mM imidazole) to elute weakly bound proteins. The p53 protein was eluted with 20 mL of Buffer D (0.3 M NaCl, 50 mM NaH₂PO₄ (pH 8.0), 20% (v/v) glycerol, 10 mM β -mercaptoethanol, 0.5 mM PMSF, 250 mM imidazole) and collected at the 250 mM imidazole absorbance (OD₂₈₀) increase. Figure 2.2 shows a

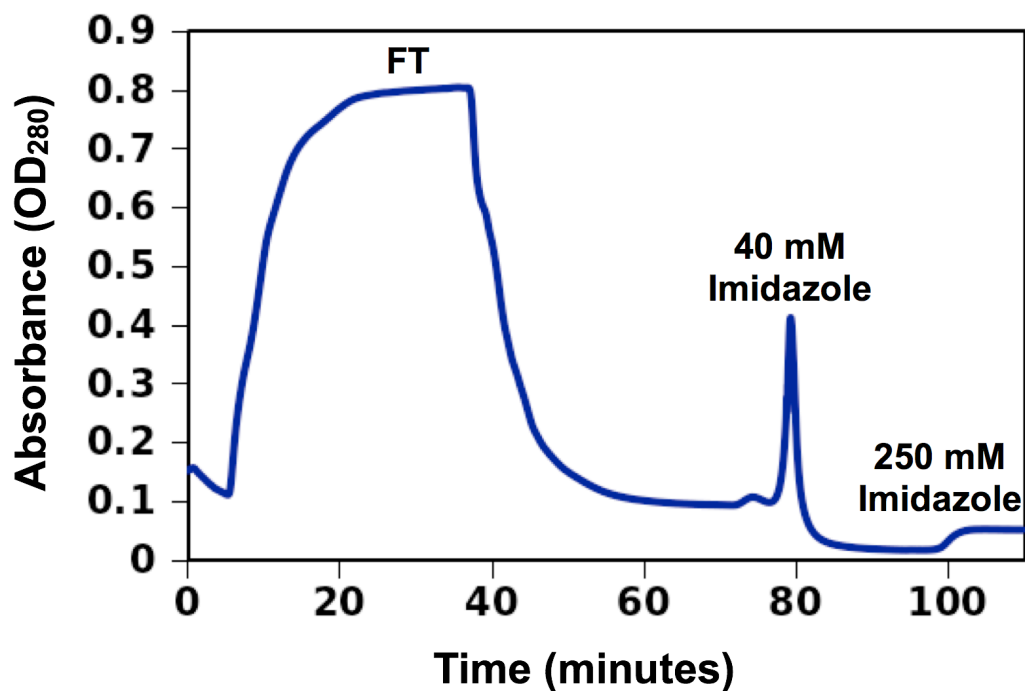


Figure 2.2. His-Tagged p53 Purification Elution Profile Schematic. The figure above is an example of the elution profile for p53 Ni-column purification. Buffer D was added to the column to elute p53 once the absorbance of Buffer C had a constant reading. The 250 mM imidazole absorbance increase is where p53 was eluted and collected. Collection of p53 began once the absorbance started to increase and till the absorbance began to level off.

schematic for p53 purification elution profile.

Following purification, eluted p53 was consecutively dialyzed, against 1 L of pre-chilled Dialysis Buffer (0.3 M NaCl, 50 mM NaH₂PO₄ (pH 8.0), 20% (v/v) glycerol, 10 mM β -mercaptoethanol) at 4 °C. Each dialysis step was for 1 hour. Dialyzed p53 was transferred to a sterile 15 mL conical tube and stored at 4 °C.

2.2.5 *Thrombin digestion*

Removal of the N-terminal 6x-histidine tag was performed by thrombin digestion. Thrombin is a serine protease with a high proteolytic specificity for the cleavage site (Leu-Val-Pro-Arg-Gly-Ser) and is commonly used in the removal of purification tags from recombinant proteins.

Upon receipt of BioUltra human thrombin from Sigma-Aldrich (St. Louis, MO) it was diluted using DNA grade sterile water to a working concentration of 1 U/ μ L and stored at -80 °C in 5 μ L aliquots. Cleavage was performed by adding 5 Units of thrombin per 1 mL of 0.01 mg/mL p53 and incubating for 2 hours at room temperature. Thrombin was inactivated by the addition of 1 mM PMSF, from freshly made 200 mM PMSF stock, and stored at 4 °C. Cleavage was confirmed by SDS-PAGE, Figure 2.3, (see section 2.3.1) and western blot analysis (see section 2.3.3).

2.3 *Protein Detection Methods*

2.3.1 *SDS-PAGE to judge sample purity*

Sodium dodecyl sulfate polyacrylamide gel electrophoresis (SDS-PAGE) was used to visualize the p53 purification steps and to determine p53 purity. SDS-PAGE is

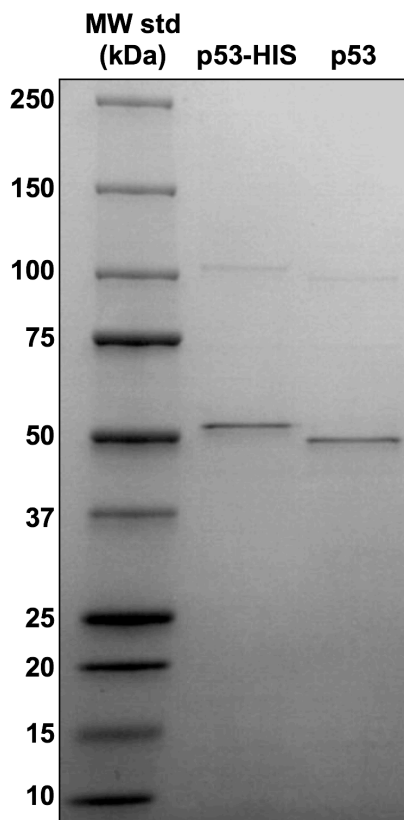


Figure 2.3. SDS-PAGE of 6x-Histidine Tag Thrombin Cleavage. The SDS-PAGE gel above shows that the band at the 50 kDa MW marker shifts down when the 6x-histidine tag is cleaved off. For visualization the gel was stained with Coomassie Blue.

performed under denaturing conditions allowing for proteins to be detected by their molecular weights (MW).⁴³ Under denaturing conditions SDS, an anionic detergent, binds to the polypeptide chain disrupting the majority of secondary, tertiary, and quaternary structures in the protein. SDS binds at an even charge-to-mass ratio giving polypeptides a negative charge, allowing for protein separation to be based on size using a polyacrylamide gel.

The different steps of purification were visualized using a 10% resolving polyacrylamide gel (4.1 mL deionized water, 3.3 mL 30% bis-acrylamide solution (29.2% (w/v) acrylamide, 0.8% (w/v) N,N' bis-methylene-acrylamide), 2.5 mL 1.5 M Tris-HCl, 0.1 mL 10% (w/v) SDS; mix and add 50 μ L 10% APS and 5 μ L tetramethylethylenediamine (TEMED) immediately before pouring gel) with a 4% stacking polyacrylamide gel (3.05 mL deionized water, 0.65 mL 30% bis-acrylamide solution, 1.25 mL 0.5 M Tris-HCl, 0.05 mL 10% (w/v) SDS; mix and add 25 μ L 10% ammonium persulfate (APS) and 5 μ L TEMED immediately before pouring gel). At each step of purification (see section 2.2.4) a 50 μ L sample was taken: lysate after sonication, insoluble (suspended in 1x PBS (137 mM NaCl, 2.7 mM potassium chloride (KCl), 1.2 mM phosphate monobasic, monohydrate (Na₂HPO₄ and KH₂PO₄) (pH 6.6)) and soluble after centrifugation, and all collections from chromatography (FT, 40 mM and 250 mM). This is shown in Figure 2.4. For each sample an 1:1 dilution was made using 2x Column Load Buffer (125 mM Tris-HCl (pH 6.8), 20% glycerol, 4% (w/v) SDS, 0.005% (w/v) bromophenol blue; 5% β -mercaptoethanol) followed by a 5 minute boil to ensure full denaturization. Gels were loaded with 5 μ L of Precision Plus Protein All Blue Standards

purchased from Bio-Rad Laboratories (Hercules, CA); 8 μ L of lysate, insoluble, soluble, and FT; and 15 μ L of the 40 mM and 250 mM imidazole elution peaks. Electrophoresis was performed using a Mini-PROTEAN Tetra Cell module with a PowerPac Universal power supply, both purchased from Bio-Rad Laboratories, in 1x TGS (25 mM Tris, 192 mM glycine, 0.1% (w/v) SDS) running buffer at a constant voltage of 100 volts for 10 minutes followed by 200 volts for 45 minutes.

Purity percentage of p53 was determined using SDS-PAGE as described above with the following changes. A 4-20% Tris-HCl Criterion pre-cast gel and Criterion Cell module from Bio-Rad Laboratories were used for electrophoresis.

For visualization, gels were stained with Coomassie Stain (45% (v/v) methanol (MeOH), 10% (v/v) glacial acetic acid, 0.25% (w/v) brilliant blue R250) for 30 minutes; and destained with Coomassie Destain (7% (v/v) MeOH, 6.5% (v/v) glacial acetic acid) for 3 hours to overnight. Examples of a p53 SDS-PAGE gel can be seen in Figure 2.4.

2.3.2 *SDS-PAGE to judge protein concentration*

Due to the low yield of purified p53 and buffer conditions, specifically β -mercaptoethanol, normal spectroscopic techniques for determining protein concentration could not be used. On the basis that coomassie blue binds basic and aromatic amino acids; and stains evenly throughout polyacrylamide gels⁴⁴, SDS-PAGE was used to estimate p53 concentration by comparison to a protein of known concentration.

Staphylococcus aureus recombinant nuclease A (SNase), another protein studied in the lab, was used as a protein concentration standard. The concentration of SNase was determined through two different spectroscopic methods: using an extinction coefficient

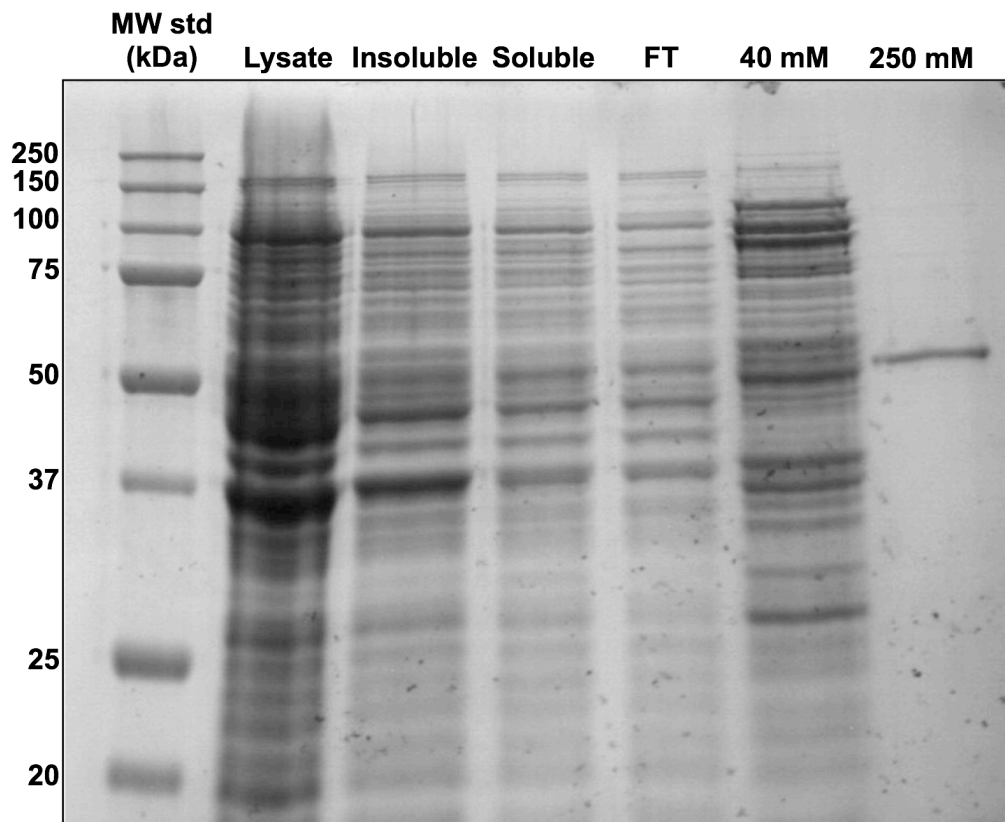


Figure 2.4. SDS-PAGE Analysis of p53 Purification Steps. The SDS-PAGE gel above shows samples collected during the different steps of purification, where at the end of the purification one dark band is seen at the 50 kDa molecular weight marker, representing p53. The lysate is the mixture after sonication; insoluble is the pellet and soluble is the supernatant after centrifugation; and FT is the flowthrough, 40 mM and 250 mM are the imidazole elutions from the nickel affinity chromatography. The 250 mM imidazole elution is where p53 will elute at. For visualization the gel was stained with Coomassie Blue.

and by a BCA Assay purchased from Thermo Fisher Scientific Inc. (Rockford, IL). SNase has an established extinction coefficient, $18064.5 \text{ M}^{-1} \text{ cm}^{-1}$, at OD_{280} .⁴⁵ Using the Beer-Lambert Law the absorbance of SNase at OD_{280} was converted to a concentration by:

$$A = \epsilon cl, \quad (2.1)$$

where A is the absorbance at OD_{280} , the ϵ extinction coefficient, the c protein concentration, and l the cuvette length.⁴⁶ The BCA Assay is a colorimetric technique using the reduction of Cu^{2+} ions to Cu^+ , by peptide bonds, which interact with bicinchoninic acid giving a purple color that absorbs at an OD_{562} .⁴⁷ Using a protein of known concentration, a standard curve was formed and used to determine the concentration of the protein. Through both of these methods, the concentration of the SNase in stock solutions was determined to be 0.744 mg/mL .

For determining p53 concentration, a SDS-PAGE was run as described above (see section 2.3.1) with the following changes. A 15% resolving polyacrylamide gel (2.4 mL deionized water, 5.0 mL 30% bis-acrylamide solution, 2.5 mL 1.5 M Tris-HCl, 0.1 mL 10% (w/v) SDS; mix and add 50 μL 10% APS and 5 μL TEMED immediately before pouring gel) with a 4% stacking polyacrylamide gel (section 2.3.1) was used. Five 10 μL SNase samples were made containing the following concentrations; 0.03 mg/mL , 0.02 mg/mL , 0.015 mg/mL , 0.01 mg/mL , and 0.0075 mg/mL . While two 10 μL p53 samples were made; undiluted p53 and a 2-fold dilution of p53 ($\frac{1}{2}$ p53). All samples were diluted 1:1 with 2x Column Load Buffer and boiled for 5 minutes. Gels were loaded with 2.5 μL of Precision Plus Protein All Blue Standard from Bio-Rad Laboratories and 15 μL of each sample. Electrophoresis was performed in 1x TGS running buffer at a constant voltage of

100 volts for 10 minutes, followed by 200 volts for 55 minutes.

After electrophoresis, the gel was stained (see section 2.3.1), imaged (see section 2.6.1) and analyzed using TotalLab Quant (see section 2.6.4). An example of a gel for judging p53 concentration can be seen in Figure 2.5.

2.3.3 *Western blot detection of p53*

Western blot analysis, the specific detection of proteins through antibody interactions⁴⁸, was used to detect the presence of p53 in purified samples. For p53 detection the monoclonal antibody DO-1, which binds to an N-terminal epitope of human p53 consistent of amino acids 11-25, from Santa Cruz Biotechnology (Santa Cruz, CA) was used.⁴⁹

The p53 protein was first subjected to SDS-PAGE (see section 2.3.1), using the 4-20% Tris-HCl Critrion pre-cast gel (Bio-Rad Laboratories) and 5 μ L of Proccession Plus Protein WesternC Standard (Bio-Rad Laboratories) as the molecular weight standard. During electrophoresis, 2 L of Towbin Transfer Buffer (25 mM Tris-base (pH 8.3), 192 mM glycine, 20% (v/v) MeOH) was chilled at 4 °C, and 2 L of TBS-T (20 mM Tris-base (pH 7.5), 0.1M NaCl, 0.1% (v/v) Tween-20) was made. After electrophoresis, both the gel and nitrocellulose membrane (Amersham Hybond ECL nitrocellulose membrane, GE Healthcare (Piscataway, NJ) were equilibrated for 10 minutes in Towbin Transfer Buffer, followed by electroblot sandwich formation. Blotting was performed using a Criterion Blotter (Bio-Rad Laboratories) and a Power Source 300V power supply (VWR) for 30 minutes at a constant voltage of 100 volts.

After blot completion, the nitrocellulose membrane was incubated in 50 mL of

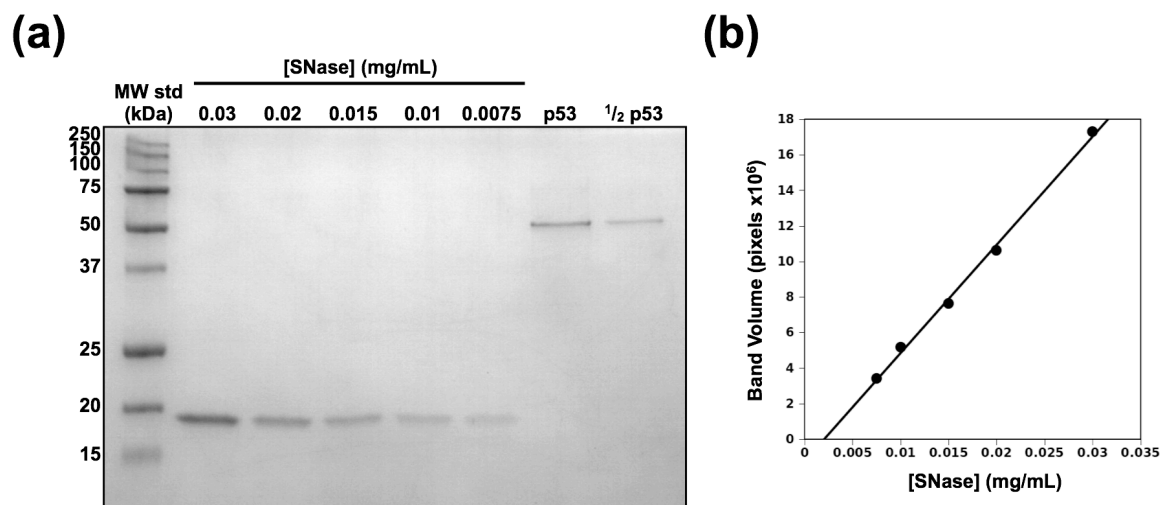


Figure 2.5. p53 Concentration Determination by SDS-PAGE. (a) An example of a SNase dilution gel done to determine the concentration of p53. (b) A standard curve made from the gel in (a) by comparing the band volumes of the SNase bands. The equation from this standard curve was used to determine the concentration of p53.

TBS-T for 5 minutes at room temperature. All three main washes, blocking, primary, and secondary antibody, were done in 50 mL of TBS-T containing 2.5 g of dry milk for 1 hour with orbital shaking at room temperature. Three wash steps, using 50 mL of TBS-T, were performed at room temperature with orbital shaking after each of the main washes. These three washes were done for 2 minutes after blocking; and for 10 minutes after both primary and secondary antibody. The primary antibody, the monoclonal antibody DO-1 from Santa Cruz Biotechnology, was used at a 1:5000 dilution, and the secondary antibody, an ECL™ anti-mouse IgG linked Horseradish Peroxidase (GE Healthcare), was used at 1:25000 dilution.

After washes, the membrane was blot dried and incubated with ECL Prime chemiluminescence (GE Healthcare) for 5 minutes. Excess ECL reagent was blotted off and the immunoreactive protein bands were visualized (see section 2.6.1). An example can be seen in Figure 2.6.

2.3.4 Glutaraldehyde cross-linking to detect oligomerization

To determine the oligomerization of p53, glutaraldehyde cross-linking was performed.⁵⁰ Glutaraldehyde reacts with primary amines, forming intra-subunit covalent bonds, allowing for oligomerization structure to be visualized by SDS-PAGE.⁵¹

Glutaraldehyde saturation was demonstrated in six reactions. These were performed in a 25 μ L volume containing 260 nM of p53 with varying amounts of freshly diluted glutaraldehyde; 0%, 0.001%, 0.005%, 0.01%, 0.05%, 0.1%. After glutaraldehyde addition, reactions were incubated at 37 °C for 5 minutes and quenched by the addition of 25 μ L of 2x Column Load Buffer and a 5 minute boil. For each reaction, 20 μ L was

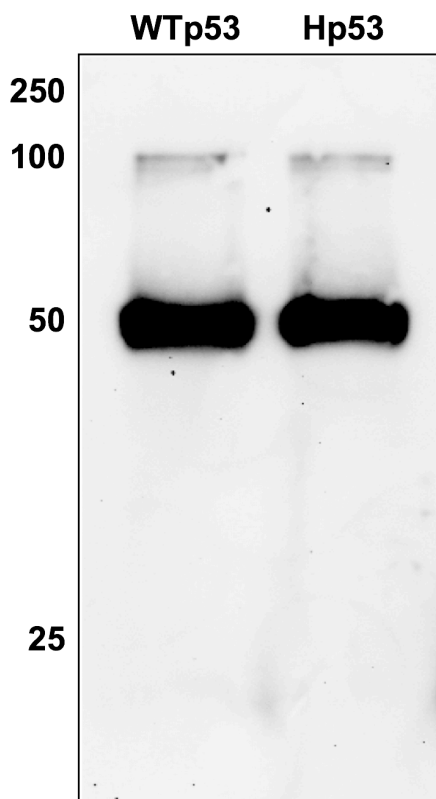


Figure 2.6. Detection of p53 through Western Blot Analysis. The gel above shows the specific binding of the monoclonal antibody DO-1 to both wild type p53 (WTp53) and hyperstable p53 (Hp53). Western blot analysis was used for detection with an ECL™ anti-mouse IgG linked Horseradish Peroxidase (GE Healthcare) as the secondary antibody.

loaded onto a 4-20% Tris-HCl Criterion pre-cast gel (Bio-Rad Laboratories) with 2.5-5 μ L of Procion Plus Protein WesternC Standard (Bio-Rad Laboratories). Electrophoresis was performed using a Criterion Cell (Bio-Rad Laboratories) and a Power Source 300V power supply (VWR) in 1x TGS running buffer at a constant amperage of 3 mA for 24 hours, 4 °C. An example can be seen in Figure 2.7.

To determine the oligomerization of p53 during EMSAs (see section 2.5), glutaraldehyde cross-linking was performed as described above but with varying concentrations of p53: 260 nM, 130 nM, and 65 nM and either 0% or 0.1% glutaraldehyde. Glutaraldehyde cross-linking was visualized using western blot analysis (see section 2.3.3).

2.4 DNA Synthesis and Sample Preparation

2.4.1 DNA synthesis

p53 recognition elements are double-stranded (dsDNA) containing two copies of a 10 bp half-site motif consisting of RRRC(A/T)(T/A)GYYY where R represents a purine base and Y a pyrimidine.⁵² To perform binding assays, two recognition elements *p21* and *PG* and two random sequences were used. Single-stranded DNA (ssDNA) sequences *PG*^{26,52}, *p21*⁵³, Random 1(R1) and Random 2 (R2) were synthesized by GeneScript (Piscataway, NJ). Upon receipt, ssDNA was dissolved in DNA grade sterile water to a working concentration of 0.5-1 mg/mL and stored at -80 °C. Figure 2.8 shows the different ssDNA nucleotide sequences used.

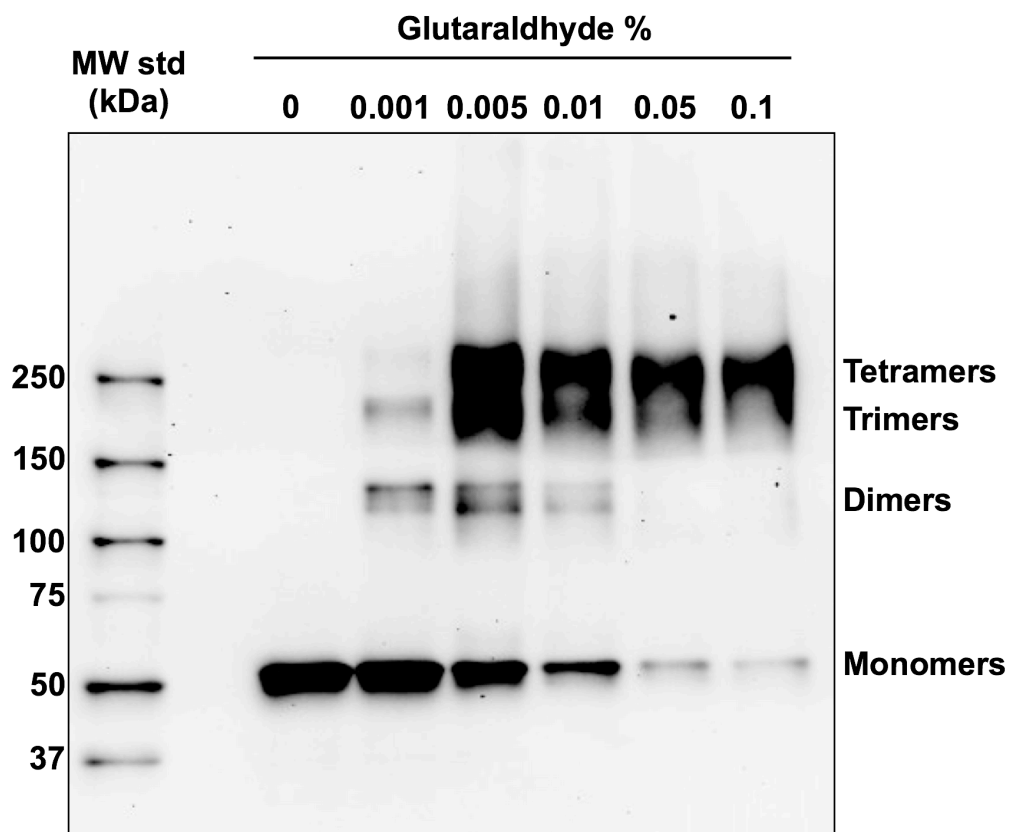


Figure 2.7. Visualization of p53 Oligomerization State by Glutaraldehyde Cross-Linking. Above is a western blot of a glutaraldehyde cross-linking that shows glutaraldehyde saturation of p53 samples. Using 0.05% and 0.1% glutaraldehyde, crosslinking showed that the majority of the p53 sample was tetramers.

- (a) **PG_{TOP}**: 5' -AGCTTAGATGCCTAGACATGCCTA-3'
- (b) **PG_{TOP}-FAM**: 5' -**FAM**-AGCTTAGATGCCTAGACATGCCTA-3'
- (c) **PG_{BOTTOM}**: 5' -AGCTTAGGCATGTCTAGGCATGTCTA-3'
- (d) **p21_{TOP}**: 5' -ATCAGGAACATGTCCCAACATGTTGAGCTC-3'
- (e) **p21_{TOP}-FAM**: 5' -**FAM**-ATCAGGAACATGTCCCAACATGTTGAGCTC-3'
- (f) **p21_{BOTTOM}**: 5' -GAGCTCAACATGTTCCACATGTTCTGAT-3'
- (g) **Random2_{TOP}**: 5' -AATATGGTTTGAATAAAGAGTAAAGATTTG-3'
- (h) **Random2_{BOTTOM}**: 5' -GTGCCAAGATCAATGCCAACCGCAGGTCCCTTAGACA-3'
- (i) **Random1_{TOP}-FaM**: 5' -**FAM**-TATGTCTAAGGGACCTGCGGTGGCATTGATCTTG-3'
- (j) **Random1_{BOTTOM}**: 5' -GTGCCAAGATCAATGCCAACCGCAGGTCCCTTAGACA-3'

Figure 2.8. Single-Stranded DNA (ssDNA) Sequences. The single-stranded sequences used to form the double-stranded recognition sequences are shown above. For forming the non-labeled dsDNA recognition sequences (a), (c), (d), (f), (g), and (h) were used. For forming the FAM-labeled dsDNA recognition sequences (b), (c), (e), (f), (i), and (j) were used.

2.4.2 Spectroscopic determination of ssDNA concentration

The concentration of ssDNA was determined by absorbance readings at OD₂₆₀ and the Oligo Calc: Oligonucleotide Properties Calculator by Northwestern University (www.basic.northwestern.edu/biotools/oligocalc.html) (Evanston, IL)⁵⁴. The Oligo Calc: Oligonucleotide Properties Calculator uses the following equation to calculate the extinction coefficients of the oligonucleotides:

$$\epsilon_S = \sum_{i=1}^{n-1} \epsilon_{N_{i,i+1}} - \sum_{i=2}^{n-1} \epsilon_i, \quad (2.2)$$

where ϵ_S is the extinction coefficient of the ssDNA; ϵ_N the nearest neighbor extinction coefficient of neighboring nucleotide i and $i+1$; and ϵ_i is the individual extinction coefficient for nucleotide. Values for the nearest neighbor and individual extinction coefficients can be seen in Tables 2.1 and 2.2. The Beer-Lambert Law (equation 2.1) was used to calculate the concentration of ssDNA; using the extinction coefficient calculated by equation 2.2 and the absorbance at OD₂₆₀.

The absorbance of the ssDNA was determined by an 1:100 dilution with DNA grade sterile water and using a DU 730 Life Science UV/Vis Spectrophotometer from Beckman Coulter (Schaumburg, IL). For both non-label and FAM-labeled ssDNA, the calculator's molecule setting was set to ssDNA and the sequence and absorbance, fixed for the dilution factor, were entered into appropriate modules. Additionally, for the FAM-labeled ssDNA the 5' modification was set to Fluorescein (6-FAM). Concentrations were recorded in microMolar (μM) amounts.

Table 2.1. The Nearest Neighbor Extinction Coefficients ($\text{L mol}^{-1} \text{ cm}^{-1}$) for the Neighboring Nucleotides i and $i+1$.

	$i = \text{dA}$	$i = \text{dT}$	$i = \text{dG}$	$i = \text{dC}$
$i+1 = \text{dA}$	27400	22800	25000	21200
$i+1 = \text{dT}$	23400	6800	19000	16200
$i+1 = \text{dG}$	25200	20000	21600	17600
$i+1 = \text{dC}$	21100	15200	18000	14600

Table 2.2. Individual Extinction Coefficient ($\text{L mol}^{-1} \text{ cm}^{-1}$) for Individual Nucleotides i .

$i = \text{dA}$	$i = \text{dT}$	$i = \text{dG}$	$i = \text{dC}$
15400	8700	11500	7400

2.4.3 *Preparation of DNA oligomers*

Using the determined concentrations of ssDNA (see section 2.4.2), at a total volume of 200-500 μL equal molar volumes of both complementary strands were mixed with Annealing Buffer (10 mM Tris (pH 7.5-8.0), 50 mM NaCl, 1 mM ethylenediaminetetraacetic acid (EDTA)). Oligomerization was performed by incubating annealing mixture at 90-95 $^{\circ}\text{C}$ for 3-5 minutes in a Thermomixer from Eppendorf (Hauppauge, NY), followed by setting the annealing mixture on the bench-top and allowing it to cool to room temperature (~45-60 minutes).

Alternatively, annealing was performed using a thermocycler. Annealing was performed by heating annealing mixture at 95 $^{\circ}\text{C}$ for 5 minutes, 46 one minute steps of -1 $^{\circ}\text{C}/\text{minute}$, 30 minutes at 55 $^{\circ}\text{C}$, and lastly 20 one minute steps of -1 $^{\circ}\text{C}/\text{minute}$.

Oligomerization was confirmed by native-PAGE, using a 15% native polyacrylamide gel (4.67 mL deionized water, 5.0 mL 30% bis-acrylamide solution, 330 μL 10x TBE (890 mM Tris, 890 mM boric acid, 20 mM EDTA (pH 8.0-8.3)); mix and add 50 μL 10% APS and 5 μL TEMED immediately before pouring gel). The annealed oligomers were compared to both complementary ssDNA. DNA gel samples were prepared by mixing 5 μL of ssDNA/dsDNA with 5 μL of Native Column Loading Buffer (0.33x TBE, 30% (v/v) glycerol; can or cannot contain 0.01% (w/v) bromophenol blue). Gels were ran in a Mini-PROTEAN Tetra Cell module (Bio-Rad Laboratories) using the PowerPac Universal power supply (Bio-Rad Laboratories). Gels were pre-electrophoresed in 0.33x TBE running buffer at 28 volts, 4 $^{\circ}\text{C}$, for 45 minutes prior to samples being loaded. After loading 10 μL of each sample, gels were electrophoresed in

0.33x TBE running buffer at 200 volts, 4 °C, for 50 minutes.

The DNA was visualized by imaging the gels, FAM-labeled DNA (see section 2.6.3) and non-labeled DNA (see section 2.6.2). An example of DNA oligomerization can be seen in Figure 2.9.

2.4.4 Spectroscopic determination of dsDNA concentration

The concentration of dsDNA was determined, as described in section 2.4.2, by absorbance readings at OD₂₆₀ and using the Oligo Calc; Oligonucleotide Properties Calculator by Northwestern University (www.basic.northwestern.edu/biotools/oligocalc.html)⁵⁴ with the following changes. To determine the extinction coefficient for dsDNA the following equation was used:

$$\epsilon_D = (1 - h_{260nm})(\epsilon_{S1} + \epsilon_{S2}), \quad (2.3)$$

$$h_{260nm} = 0.287 f_{AT} + 0.059 f_{GC}, \quad (2.4)$$

where ϵ_D is the extinction coefficient of the dsDNA; ϵ_{S1} and ϵ_{S2} are the extinction coefficients for the ssDNA complementary strands; h_{260nm} a correction for the hypochromic effect; f_{AT} and f_{GC} are the fractions of nucleotide base pairs (AT, GC).

The absorbance of the dsDNA was determined by an 1:100 dilution with DNA grade sterile water and using a DU 730 Life Science UV/Vis Spectrophotometer (Beckman Coulter). For both non-labeled and FAM-labeled dsDNA, the calculator's molecule setting was set to dsDNA and the top sequence and absorbance, fixed for the dilution factor, were entered into appropriate modules. Additionally, for the FAM-labeled

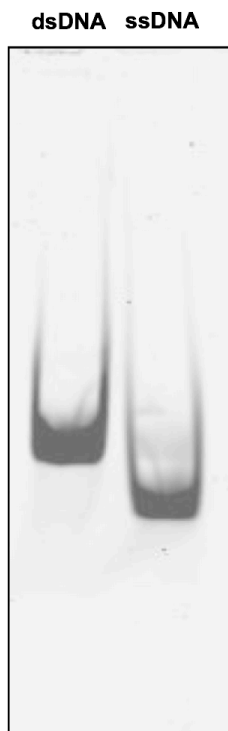


Figure 2.9. Visualization of dsDNA Oligomerization. The native gel above shows that during the DNA oligomerization the detectable majority of FAM-labeled ssDNA annealed, forming dsDNA. A native gel, stained with SYBR-gold, was also performed to show that the detectable majority of non-labeled ssDNA annealed during DNA oligomerization; this gel is not shown.

dsDNA the 5'-modification was set to Fluorescein (6-FAM). Concentrations were recorded in microMolar (μM) amounts. The dsDNA recognition sequences that were formed can be seen in Figure 2.10.

2.5 *Detection of p53:DNA Binding*

2.5.1 *EMSA using dsDNA and SYBR-gold*

To visualize p53:DNA binding activity, electrophoretic mobility shift assays (EMSA) were performed. EMSAs are an electrophoretic technique used to study protein-DNA interactions where the DNA is labeled for visualization. Since the DNA is a small molecule it migrates quickly in the native gel and as protein binds the DNA an upward shift in the band is seen due to a larger complex being formed (i.e., the protein:DNA complex).^{26,55}

DNA binding reactions were done in 30 μL volumes containing DNA Binding Buffer (0.3 M NaCl, 50 mM NaH_2PO_4 (pH 8.0), 20% (v/v) glycerol, 10 mM β -mercaptoethanol), 2 ng of recognition sequence (*p21*, *PG*, *R2*), 40 ng of competitor DNA (pBR322), 0.1 g/L BSA and p53, at varying concentrations. To see binding curves, serial dilutions of p53 were done before being added to the DNA binding reactions. Upon the addition of p53, a quick, 10 second, 10,000 x g spin was performed and reactions were incubated at 4°C for 30 minutes. While reactions were prepared and incubated, a 4-20% TBE Criterion pre-cast gel (Bio-Rad Laboratories) was pre-electrophoresed in 0.33x TBE running buffer for 45 minutes at 28 volts, 4 °C. After incubations, 25 μL of the DNA binding reactions were loaded and electrophoresed in

(a) Non-Labeled dsDNA:

PG: 5' -AGCTTAGACATGCCTAGACATGCCTA-3'
3' -ATCTGTACGGATCTGTACGGATTCGA-5'

p21: 5' -ATCAGGAACATGTCCCAACATGTTGAGCTC-3'
3' -TAGTCCTTGTACAGGGTTGTACAACTCGAG-5'

R2: 5' -AATATGGTTTGAATAAAGAGTAAAGATTTG-3'
3' -TTATACCAAACCTATTTCTCATTTCTAAAC-5'

(b) FAM-Labeled dsDNA:

PG: 5' -**FAM**-AGCTTAGACATGCCTAGACATGCCTA-3'
3' -ATCTGTACGGATCTGTACGGATTCGA-5'

P21: 5' -**FAM**-ATCAGGAACATGTCCCAACATGTTGAGCTC-3'
3' -TAGTCCTTGTACAGGGTTGTACAACTCGAG-5'

R1: 5' -**FAM**-TATGTCTAAGGGACCTGCGGTTGGCATTGATCTTG-3'
3' -ACAGATTCCCTGGACGCCAACCGTAACCTAGAACCGTG-5'

Figure 2.10. Double-Stranded DNA (dsDNA) Sequences. (a) Shows the dsDNA recognition sequences that were made and used for non-labeled DNA experiments. (b) Shows the dsDNA recognition sequences that were made and used for the FAM-labeled DNA experiments.

0.33x TBE running buffer for 1 hour and 40 minutes at 200 volts, 4 °C. Upon completion of electrophoresis, gels were imaged (see section 2.6.2) and analyzed (see section 2.6.5).

2.5.2 EMSA using dsDNA with FAM-label

DNA binding reactions were done in 30 µL volumes containing DNA Binding Buffer (see section 2.2), 2 ng of recognition sequence DNA (*p21*, *PG*, *R1*), 40 ng of competitor DNA (salmon sperm), 0.1 g/L BSA and p53, at varying concentrations. Due to degradation of dsDNA over time, the recognition sequence was heated at 90 °C for 2 minutes and allowed to cool for 30 minutes, room temperature. To see binding curves, serial dilutions of p53 were done before being added to DNA binding reactions. Upon the addition of p53, a quick, 10 second, 10,000 x g spin was performed and reactions were incubated for 30 minutes, 4 °C. While reactions were prepared and incubated, a 4-20% TBE Critrion pre-cast gel (Bio-Rad Laboratories) was pre-electrophoresed in 0.33x TBE running buffer for 45 minutes at 28 volts, 4 °C. After incubation, 25 µL of the DNA binding reactions were loaded and electrophoresed in 0.33x TBE running buffer for 1 hour and 40 minutes at 200 volts, 4 °C. Upon completion of electrophoresis, gels were imaged (see section 2.6.3) and analyzed (see section 2.6.5). An example of an EMSA can be seen in Figure 2.11.

2.6 Gel Imaging and Analysis

2.6.1 Imaging of Coomassie stained protein gels and western blots

Coomassie stained protein gels were either imaged using a FOTO/Analyst FX

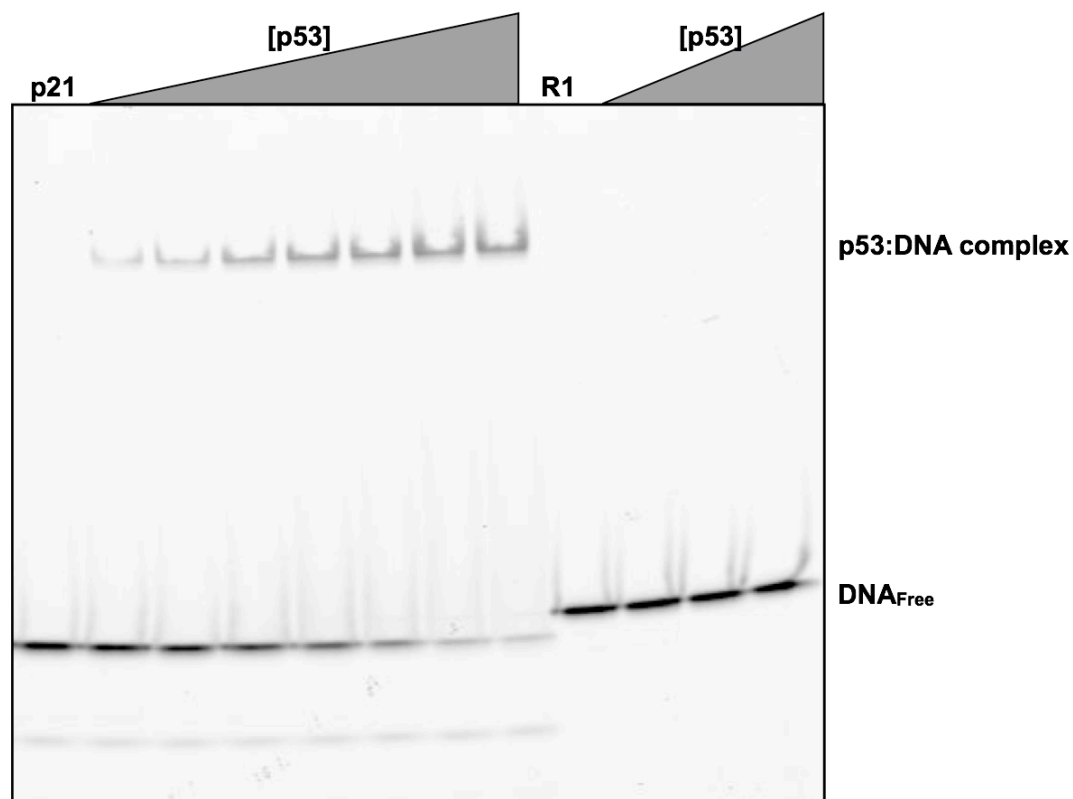


Figure 2.11. Example of EMSA Using FAM-Labeled dsDNA. The native gel above is an example of an EMSA using FAM-labeled dsDNA, where the bottom bands represent the free dsDNA and the top bands are the p53:DNA complex. The left side of the gel shows specific binding of p53 for p21, a known recognition element. While the right side shows that no detectable non-specific p53 binding occurred using a random dsDNA sequence, R1.

imager from Fotodyne, Inc. (Hartland, WI) or a red imager from Alpha Innotech (Santa Clara, CA).

When imaging coomassie stained protein gels with the FOTO/Analyst FX imager, the gel was placed on the electroluminescent (EL) visible light panel and imaged using the coomassie blue filter. If Imaged with the red Imager, the gel was placed on the sample tray and imaged using the white light setting.

Western blots were imaged with the FOTO/Analyst FX imager. The nitrocellulose membrane was centered on the Lumi/Tray. The filter was set to the Close-Up adaptor with a fully open iris and auto focused. Five exposures were performed: 11 seconds, 1.11 minutes, 2.22 minutes, 3.33 minutes, and 11.11 minutes.

2.6.2 Imaging of SYBR-gold stained DNA

SYBR-gold stained gels were imaged using the Typhoon Trio Variable Mode imager. The gels were first stained in 50 mL of SYBR-gold stain (0.33x TBE, 0.01% SYBR-Gold from Invitrogen (Eugene, OR)) for 30 minutes with orbital rotation at room temperature. The gel was then placed on the glass platen of the Typhoon Trio and air bubbles were rolled out. On the grid of the scanner control window, the gel scan area was selected and the acquisition mode was set to fluorescence. In the setup window, the emission filter was set to 580 BP 30 Cy3, TAMRA, AlexaFluor546, and laser to green. Appropriate image orientation was chosen and pixel size was set to 200 microns.

2.6.3 Imaging of FAM-labeled DNA

Gels containing FAM-labeled DNA were imaged using the Typhoon Trio Variable

Mode imager. After the gels were placed on the glass platen of the Typhoon Trio and air bubbles rolled out, the gel scan area was selected on the grid of the scanner control window and the acquisition mode set to fluorescence. In the setup window, the emission filter was set to 580 BP 40 Cy2, ECI + Blue FAM, and laser to blue. Appropriate image orientation was chosen and pixel size set to 200 microns.

2.6.4 Analysis of gel images for protein concentration

Protein concentration gels were analyzed using TotalLab Quant by TotalLab Limited (Newcastle, England). Once images were loaded, lanes were created manually. Lane widths were set to that of the widest band and grimages were added for the lane and band correction. The rolling ball background subtraction with 100 radius was used to remove background noise and band detection was performed using 10% peak percentage.

Using gnumeric by GNOME (projects.gnome.org/gnumeric/), a standard curve comparing the SNase concentration (mg/mL) and the band volume (pixels) was made. Using the standard curve equation and the determined p53 band volume, the concentration (mg/mL) of p53 was calculated. For determining molarity (nM), the mg/mL concentration was divided by p53's molecular weight (hyperstable = 42424.3485 g/mol, wild type = 42421.3937 g/mol). An example of this can be seen in Figure 2.6.

2.6.5 Analysis of gel images for protein:DNA binding

EMSA gels were analyzed using TotalLab Quant (TotalLab Limited). Once images were loaded, lanes were created manually. Lane widths were set to that of the widest band and grimages were added for lane and band correction. The rolling ball

background subtraction was used with a 100 radius and bands were detected using a 10% peak percentage.

Binding curves were formed as previously described⁵⁶⁻⁵⁷ using gnumeric (GNOME). The concentration of p53 bound DNA [p53-DNA] was determined using the following equations:

$$DNA_{Free}\% = \frac{Band\ Volume\ DNA_{Free}}{Band\ Volume\ DNA_{Total}}, \quad (2.5)$$

$$DNA_{Bound}\% = 1 - DNA_{Free}\%, \quad (2.6)$$

$$[p53 - DNA] = [DNA_{Total}] * DNA_{Bound}\%, \quad (2.7)$$

where *Band Volume DNA_{Free}* is the DNA_{Free} band volume in lanes containing p53, *Band Volume DNA_{Total}* is the DNA_{Free} band volume in the lane not containing p53, *DNA_{Free}%* is the percentage of free DNA in lanes containing p53, *DNA_{Bound}%* is the percentage of DNA bound by p53 in lanes containing p53.

A binding curve was formed by comparing the p53 concentration [p53] (nM) to the concentration of p53 bound DNA [p53-DNA] (nM). The data was fit to a nonlinear least-squares regression.

A scatchard plot was also formed as previously described.⁵⁶⁻⁵⁷ This was done by comparing the percentage of p53 bound DNA [p53-DNA]/[DNA_{Total}] to the percentage of p53 bound DNA divided by the concentration of p53 [p53-DNA]/[DNA_{Total}][p53]. Data was fit to a linear regression.

CHAPTER III

RESULTS AND DISCUSSION

3.1 *Purification of Recombinant p53 and Thrombin Cleavage*

Recombinant human p53s, WTp53 and Hp53, were expressed in the soluble form using *E. coli* (Chapter 2, section 2.3) and purified by Ni⁺ affinity chromatography (Chapter 2, section 2.4). The purity of p53 was judged to be ~80% pure by Coomassie staining of samples in a SDS-PAGE gel (Chapter 2, section 3.1), Figure 3.1.

The thrombin cleavage of the 6x-histidine tag from the recombinant human p53s, WTp53 and Hp53, was confirmed by SDS-PAGE (Chapter 2, section 2.5), Figure 2.3. The identity of purified WTp53 and Hp53, with and without the 6x-histidine tag, were verified by western blot analysis using the monoclonal DO-1 (Chapter 2, section 3.3), Figure 2.6.

3.2 *Determination of p53 Oligomerization*

Under physiological conditions p53 binds recognition elements as a tetramer.^{50,53} To test p53's ability to form this tetrameric state, varying concentrations of p53 (260 nM, 130 nM, 65 nM) and glutaraldehyde (0%, 0.001%, 0.005%, 0.01%, 0.05%, 0.1%) were mixed together as described in Chapter 2, section 4.4. Through these glutaraldehyde

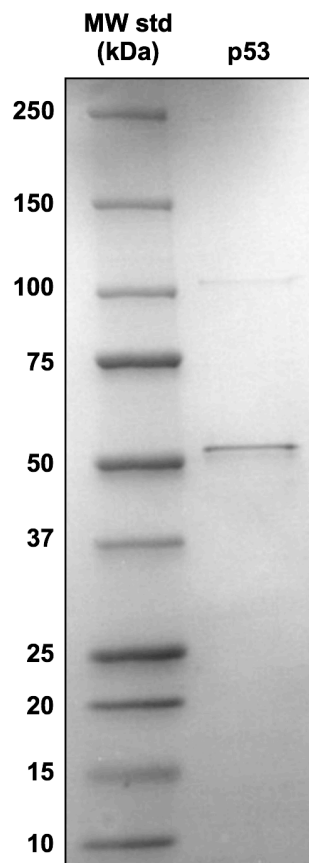


Figure 3.1. SDS-PAGE of p53 Purity After Purification. In the SDS-PAGE gel above it can be seen that there is one intense band at the 50 MW marker and one fainter band at the 100 MW marker. This gel was stained using Coomassie blue and the p53 sample was found to be ~80% pure.

cross-linkings the oligomeric state of p53 was determined for all forms: two wild type forms, WTp53-His (MRGSHHHHHHSSGLVPRGS-p53(1-363)) and WTp53 (GS-p53(1-363)); and two hyperstable forms, Hp53-His (MRGSHHHHHHSSGLVPRGS-p53(1-363(M133L/V203A/N239Y/N258D))) and Hp53 (GS-p53(1-363(M133L/V203A/N239Y/N258D))). Both, WTp53-His and Hp53-His, contain an N-terminal 6x-histidine tag and thrombin cleavage site.

The glutaraldehyde cross-linking for WTp53-His can be seen in Figure 3.2. Looking at the first six reactions of the cross-linking it's seen that as the glutaraldehyde concentration increases; dimers, trimers, tetramers, and oligomeric aggregates were formed. At different concentrations of p53 the majority seemed to be a trimer, tetramer, or an oligomeric aggregate. Suggesting that under the conditions of 0.3 M NaCl, 50 mM NaH₂PO₄ (pH 8.0), 20% (v/v) glycerol, and 10 mM β -mercaptoethanol, WTp53-His does not form tetramers exclusively.

The glutaraldehyde cross-linking for WTp53 can be seen in Figure 3.3. As with WTp53-His, as glutaraldehyde concentration increases; dimers, trimers, tetramers, and oligomeric aggregates were formed. Though when looking at varying p53 concentrations, oligomeric aggregates seemed to form less and the majority of p53 was found as trimers and tetramers. The presence of oligomeric aggregates at high glutaraldehyde concentrations suggest that WTp53 doesn't form tetramers exclusively under these conditions: 0.3 M NaCl, 50 mM NaH₂PO₄ (pH 8.0), 20% (v/v) glycerol, and 10 mM β -mercaptoethanol.

The glutaraldehyde cross-linking for Hp53-His can be seen in Figure 3.4. As seen

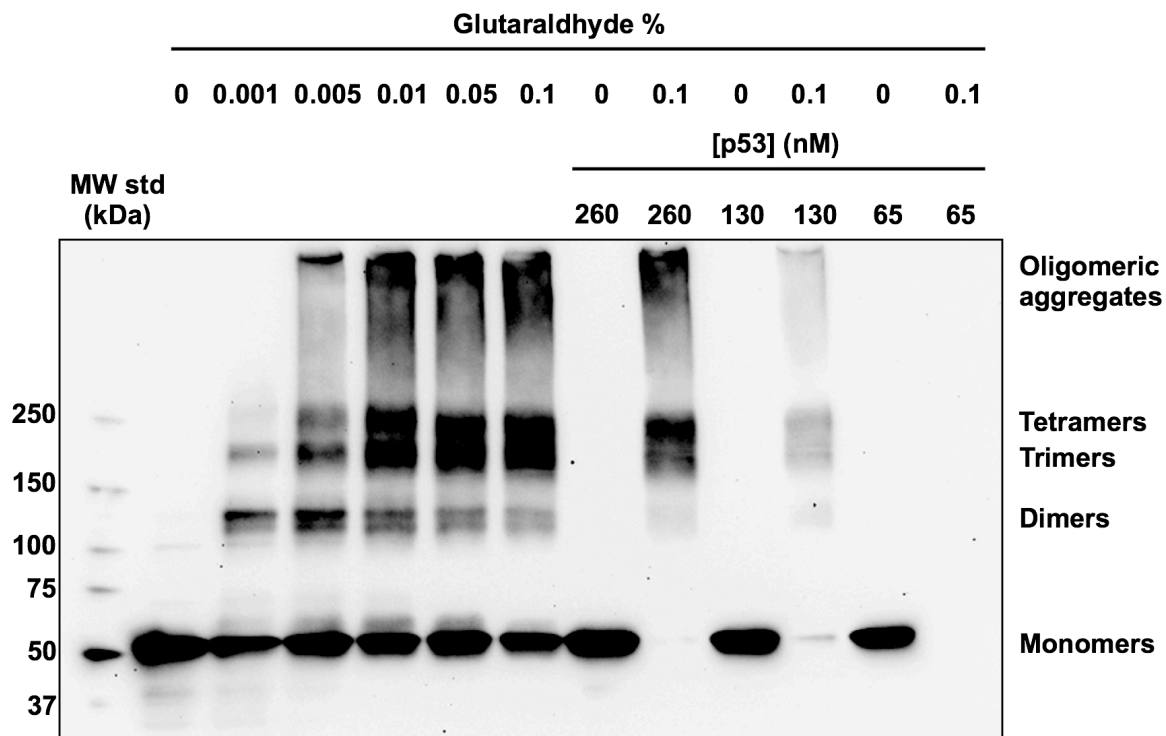


Figure 3.2. Oligomerization of Wild Type p53-His (WTp53-His) by Glutaraldehyde Cross-Linking. In the western blot above the monomers are at the MW marker 50 kDa, dimers at 100 kDa, trimers at 150 kDa, tetramers ~200 kDa, and oligomeric aggregates all above the 250 kDa marker. It is seen that as the amount of glutaraldehyde increases so does the intensity of the tetramer band, also two species of dimer can be seen. When looking at the different concentrations of p53 all oligomeric states can be seen.

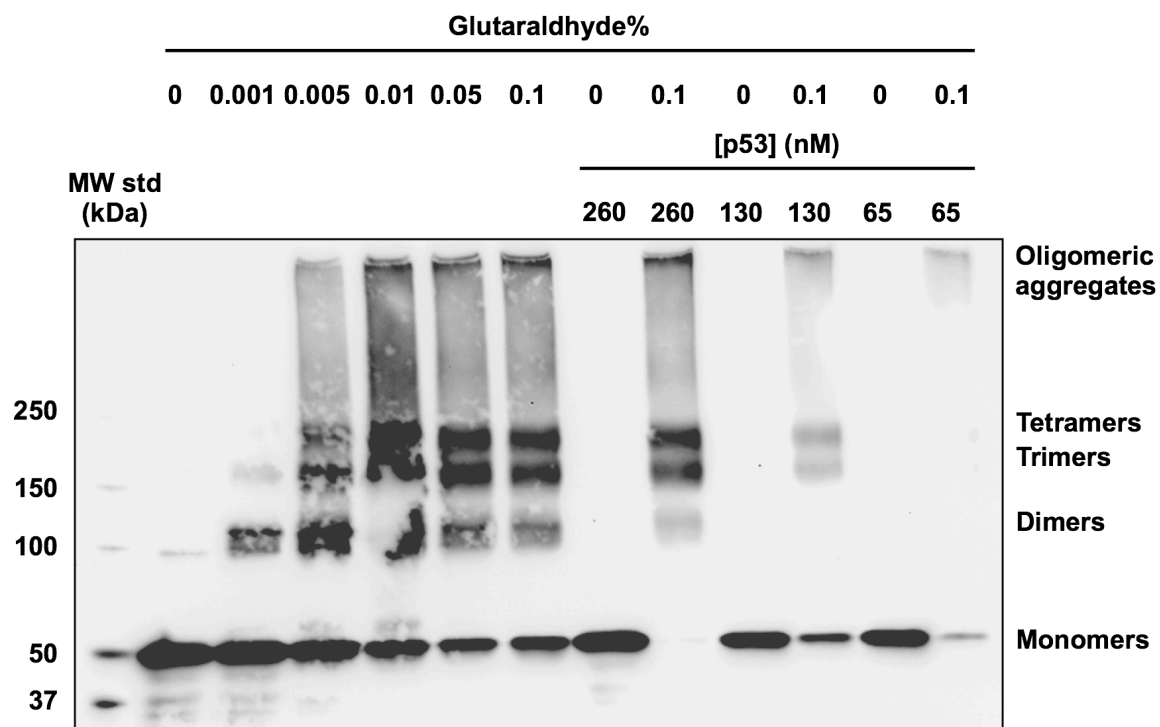


Figure 3.3. Oligomerization of Wild Type p53 (WTp53) by Glutaraldehyde Cross-Linking. In the western blot above the monomers are at the MW marker 50 kDa, dimers at 100 kDa, trimers at 150 kDa, tetramers ~200 kDa, and oligomeric aggregates all above the 250 kDa marker. It is seen that as the amount of glutaraldehyde increases so does the intensity of the tetramer band, also two species of dimer can be seen. When looking at the different concentrations of p53 all oligomeric states can be seen. Though WTp53 does seem to show less formation of oligomeric aggregates.

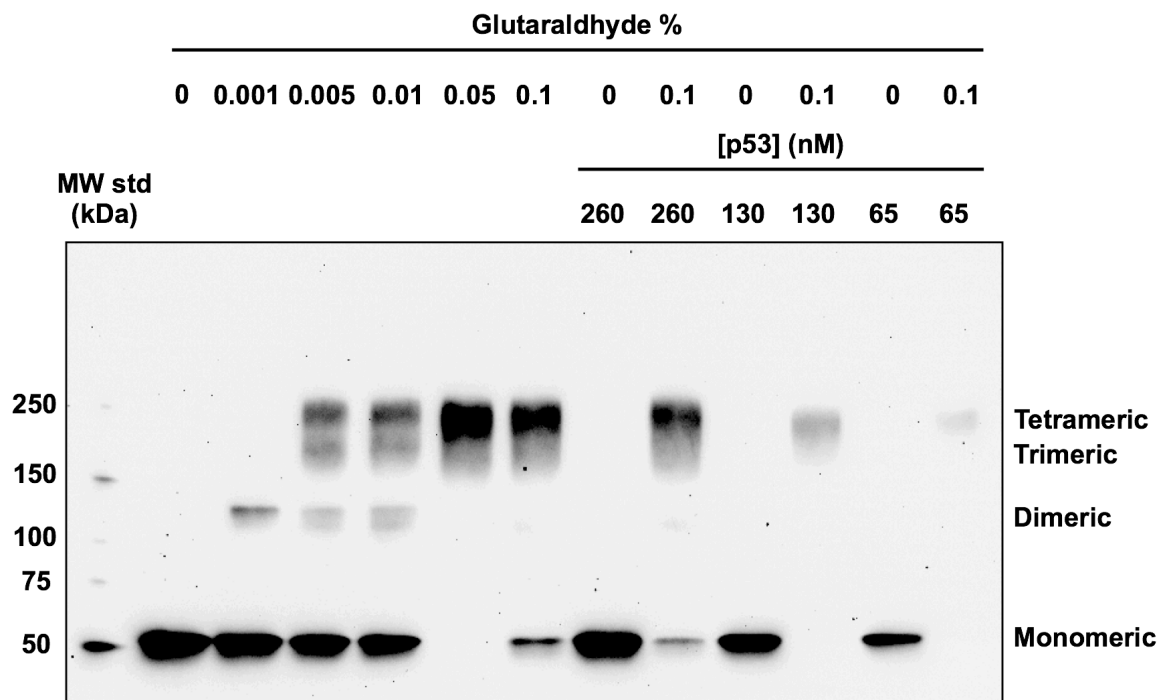


Figure 3.4. Oligomerization of Hyperstable p53-His (Hp53-His) by Glutaraldehyde Cross-Linking. In the western blot above the monomers are at the MW marker 50 kDa, dimers at 100 kDa, trimers at 150 kDa, and tetramers ~200 kDa,. Its seen that as the amount of glutaraldehyde increases so does the intensity of the tetramer band, also two species of dimer can be seen. When looking at the different concentrations of p53 the predominant oligomeric species seen is the tetrameric.

with wild type p53, higher concentrations of glutaraldehyde produced dimers, trimers and tetramers; but no oligomeric aggregates were detected. At the highest concentration of glutaraldehyde the dominant state was tetrameric. This was seen at varying p53 concentrations suggesting that Hp53-His formed stable tetramers under the tested experimental conditions.

The glutaraldehyde cross-linking for Hp53 can be seen in Figure 3.5. With increasing glutaraldehyde concentration Hp53 formed dimers, trimers, and tetramers; but, as with Hp53-His, no oligomeric aggregates were detected. At the three p53 concentrations tested the tetrameric form seemed to be favored. This suggest that Hp53 formed stable tetramers under the experimental conditions tested.

3.3 *Determination of p53 Energetic Binding Constant*

In response to cellular stresses p53 can transactivate multiple recognition elements, depending on which elements are transactivated different cellular pathways are initiated. These recognition elements are dsDNA sequences, ~20 bp, that contain two half-sites p53 binds. To determine the binding energetics for recognition elements *p21* and *PG*, electrophoretic mobility shift assays (EMSA) were done using all p53 forms, WTp53-His, WTp53, Hp53-His, and Hp53, as described in Chapter 2, section 5. These EMSAs were then analyzed (Chapter 2, section 6.6) and used to determine the K_d by transforming the binding curve into a Scatchard plot.⁵⁶⁻⁵⁷ The Scatchard plot was formed using the equation:

$$\frac{[p53-DNA]}{[DNA_{Total}][p53]} = -\left(\frac{1}{K_d}\right)\frac{[p53-DNA]}{[DNA_{Total}]} + \frac{n}{K_d} \quad (3.1)$$

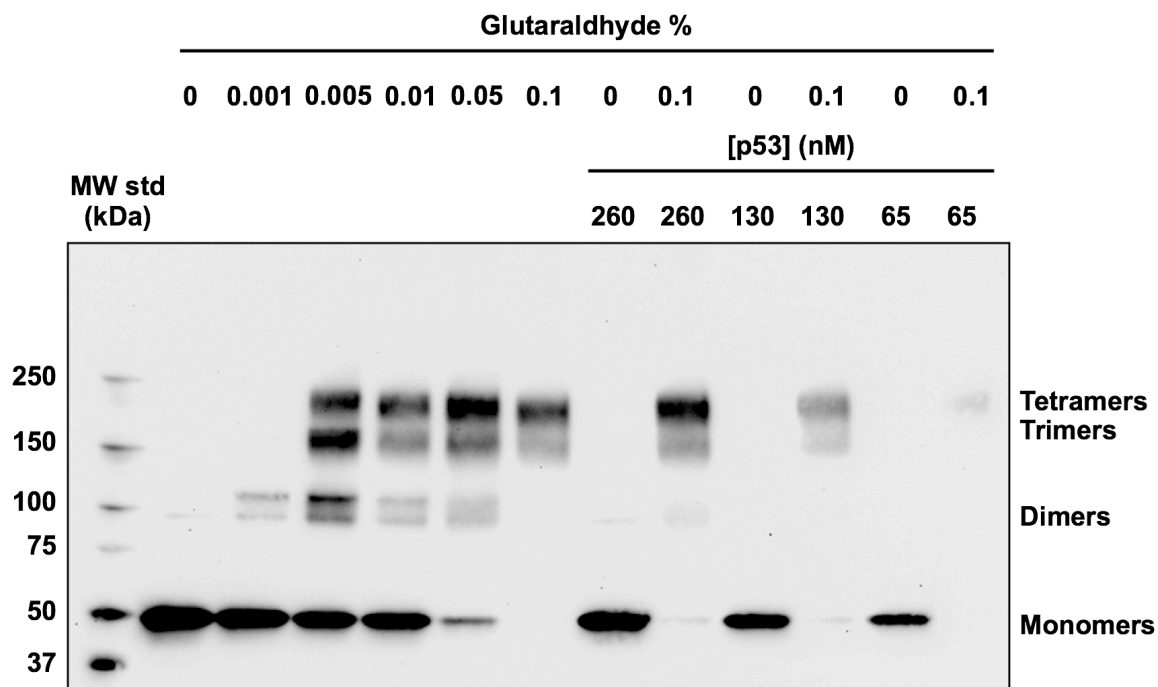


Figure 3.5. Oligomerization of Hyperstable p53 (Hp53) by Glutaraldehyde Cross-Linking. In the western blot above the monomers are at the MW marker 50 kDa, dimers at 100 kDa, trimers at 150 kDa, and tetramers ~200 kDa,. Its seen that as the amount of glutaraldehyde increases so does the intensity of the tetramer band, also two species of dimer can be seen. When looking at the different concentrations of p53 the predominant oligomeric species seen is the tetrameric.

$$\frac{r}{[L]} = -\left(\frac{1}{K_d}\right)r + \frac{n}{K_d} \quad (3.2)$$

where r is the ratio of bound DNA to total DNA ($[\text{p53-DNA}]/[\text{DNA}_{\text{Total}}]$), $[L]$ is the concentration of p53 ($[\text{p53}]$), K_d is the dissociation constant, and n is the number of binding sites for p53. This linearizes the data making K_d equal to the negative reciprocal of the line's slope.

To insure the FAM-label wouldn't affect the binding energetics, a control using non-labeled dsDNA and SYBR-gold stain was preformed as described in Chapter 2, section 5.1. All conditions were kept the same except that binding reactions used non-labeled DNA and pBR322 as the competitor DNA instead of salmon sperm. This control was preformed using Hp53-His. An EMSA and analysis of the non-labeled DNA control can be seen in Figure 3.6. In Figure 3.6 (a) as the concentration of p53 increased the band shifted upward, the DNA_{free} band disappeared as a p53:DNA complex band appeared. In comparison p53 showed a much higher affinity for *p21* and *PG* over R1. Figure 3.6 (b) and (c) show the binding curves and scatchard plots formed for recognition elements *p21* and *PG* from the gel in (a). The K_d determined for the non-labeled DNA control can be seen in Table 3.1.

The second control was a thrombin control, insuring that the addition of thrombin, for cleavage of the 6x-histidine tag, wouldn't affect the binding energetics. This was done by mixing 5 U BioUltra human thrombin with freshly made 100 mM PMSF and allowing it to incubate on ice for 5-10 minutes. It was then added to the p53 sample and EMSA's were performed and analyzed as described in Chapter 2, section 5.2. This control was

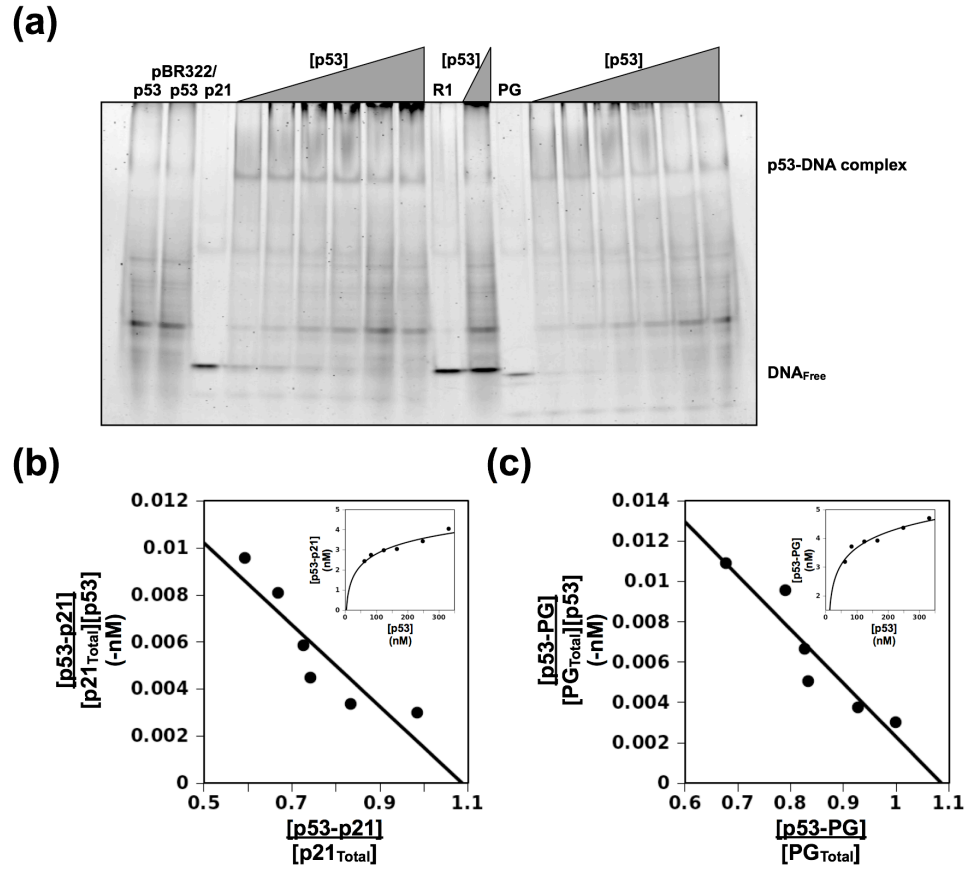


Figure 3.6. Binding Kinetics of Non-Labeled dsDNA Control for Recognition Sequences p21 and PG by EMSA. (a) Shows that EMSA done for the non-labeled dsDNA control. Since using SYBR-gold, all DNA will be seen so the first two lanes were used as controls: 1) purified p53 and 2) has the addition of pBR322. For both *p21* and *PG* the DNA_{free} band towards the bottom of the gel disappears, while a band towards the top begins to appear, p53:DNA complex, with the addition of p53. This shows specific binding since Random 2 is not being a bound at the highest concentrations of p53. (b) Shows the binding curve, inner box, and scatchard plot, outer box, for recognition element *p21*. (c) Shows the binding curve, inner box, and scatchard plot, outer box, for the recognition element *PG*.

done using Hp53-His and can be seen in Figure 3.7. In Figure 3.7 (a) as the concentration of p53 increased the p53:DNA complex band intensified. Figure 3.7 (b) and (c) show the binding curves and the scatchard plots for the gel in (a). The calculated K_d for the thrombin control can be seen in Table 3.1.

The K_d 's for WTp53-His and WTp53 were determined as described in Chapter 2, section 5.2. An EMSA of these can be seen in Figure 3.8 (a), WTp53-His, and Figure 3.9 (a), WTp53. Both showed a steady increase of the p53:DNA complex band and specific binding for the recognition sequences. The analysis for both WTp53-His and WTp53 can be seen in Figure 3.8 and Figure 3.9, (b) *p21* and (c) *PG*. For both p53 appeared to bind *PG* with higher affinity than *p21*, ~2-fold. Both, WTp53-His and WTp53, experiments were done in triplicate; K_d 's can be seen in Table 3.1.

The K_d 's for Hp53-His and Hp53 were determined as described in Chapter 2, section 5.2. Their EMSAs can be seen in Figures 3.10 (a) and 3.11 (a). Both, Hp53-His and Hp53, came close to full saturation for *p21* and *PG*. The binding energetics analysis of Hp53-His and Hp53 can be seen in the (b) *p21* and (c) *PG* of the Figures 3.10 and 3.11. The K_d 's are shown in Table 3.1. Hp53-His and Hp53 were done in triplicate for both *p21* and *PG*.

The K_d values in Table 3.1 suggest that the FAM-label and thrombin don't affect p53:DNA binding energetics. Both forms of wild type p53, WTp53-His and WTp53, had larger K_d values than what's been seen in previous research.⁵¹⁻⁵² This could possibly be due to the significant presence of oligomeric aggregates during the glutaraldehyde cross-linking, Figures 3.3 and 3.4. Both also had rather large deviations between the triplicates.

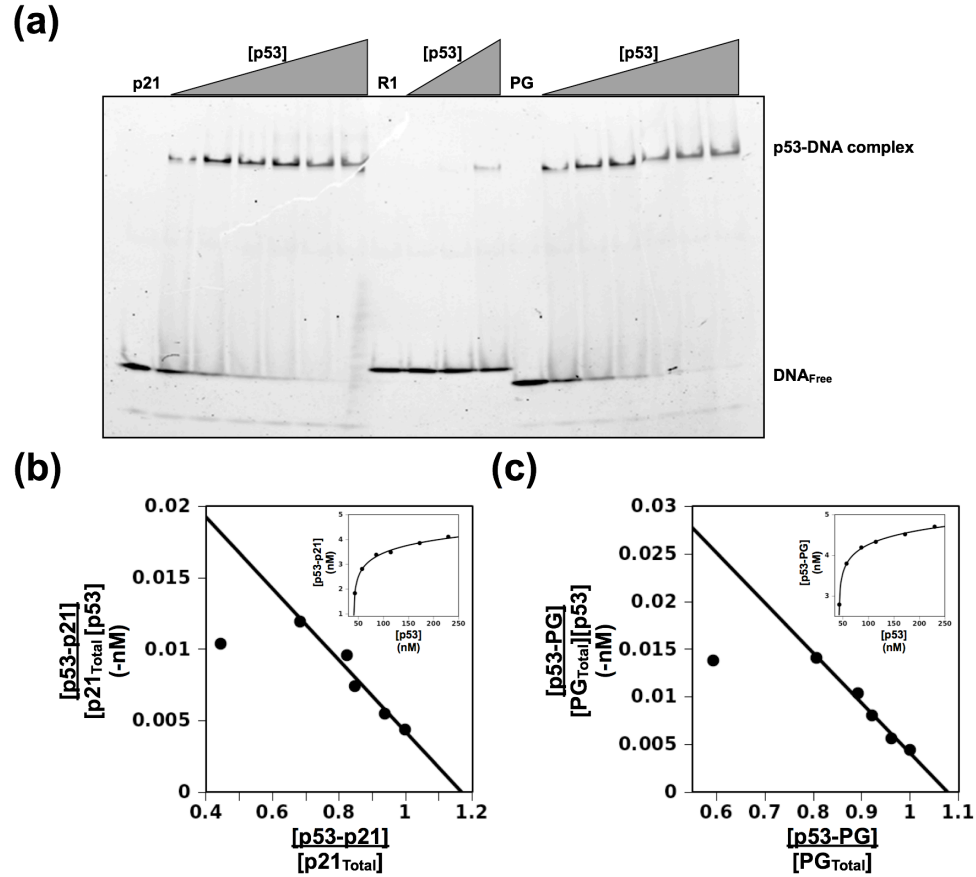


Figure 3.7. Binding Kinetics of Thrombin Control for Recognition Sequences p21 and PG by EMSA. (a) Shows that EMSA done for thrombin control. For both *p21* and *PG* the DNA_{free} band towards the bottom of the gel disappears, while a band towards the top begins to appear, p53:DNA complex, with the addition of p53. This shows specific binding since Random 1 is not being bound at the highest concentrations of p53. (b) Shows the binding curve, inner box, and scatchard plot, outer box, for recognition element *p21*. (c) Shows the binding curve, inner box, and scatchard plot, outer box, for the recognition element *PG*.

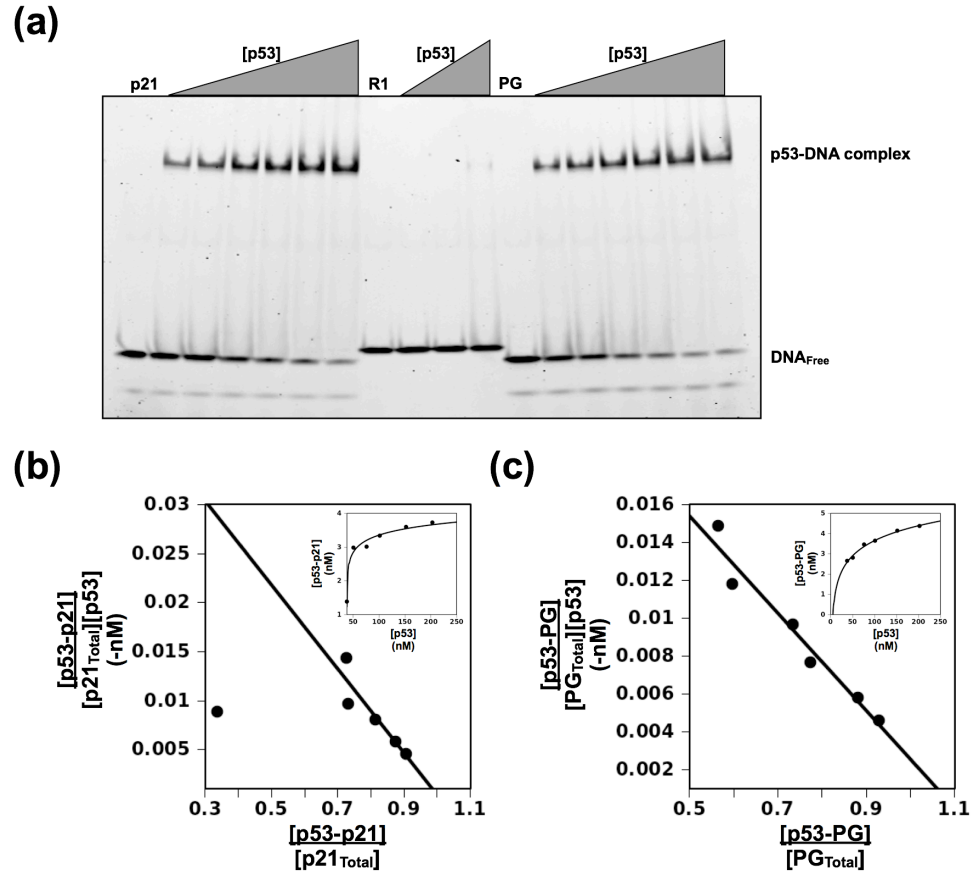


Figure 3.8. Binding Kinetics of Wild Type p53-His for Recognition Sequences p21 and PG by EMSA. (a) Shows that EMSA done for WTp53-His. For both *p21* and *PG* the DNA_{free} band towards the bottom of the gel disappears, while a band towards the top begins to appear, p53:DNA complex, with the addition of p53. This shows specific binding since Random 1 is not being a bound at the highest concentrations of p53. (b) Shows the binding curve, inner box, and scatchard plot, outer box, for recognition element *p21*. (c) Shows the binding curve, inner box, and scatchard plot, outer box, for the recognition element *PG*.

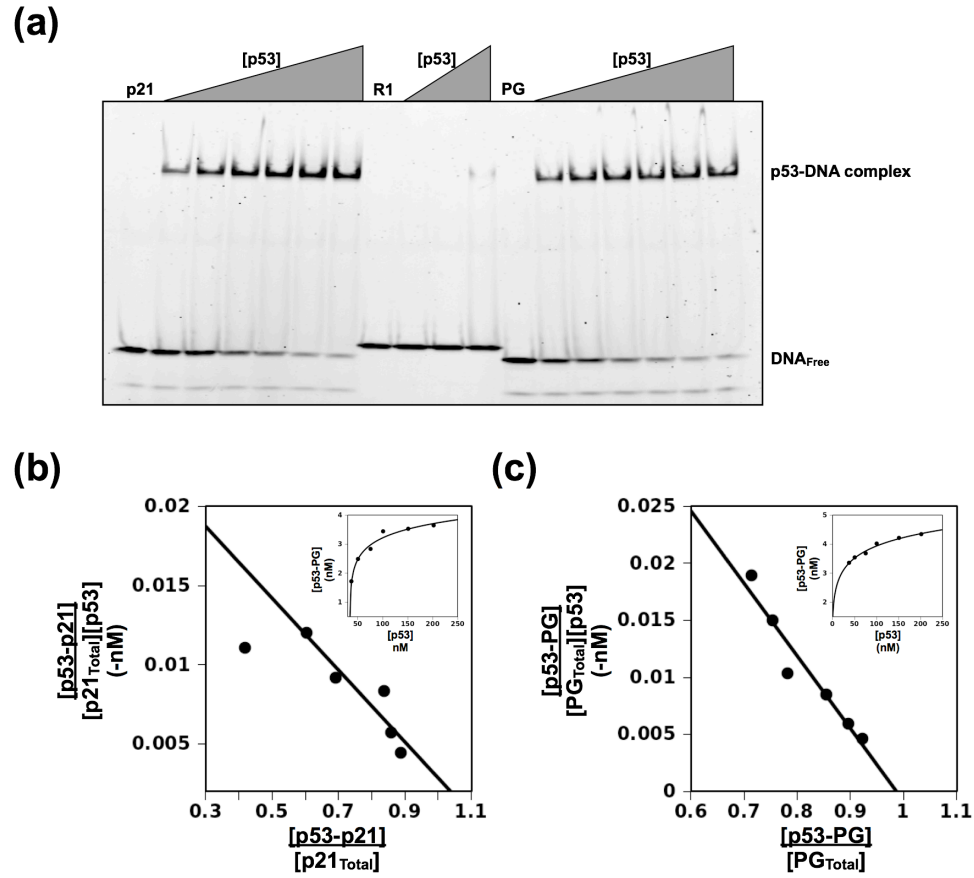


Figure 3.9. Binding Kinetics of Wild Type p53 for Recognition Sequences p21 and PG by EMSA. (a) Shows that EMSA done for WTp53. For both *p21* and *PG* the DNA_{free} band towards the bottom of the gel disappears, while a band towards the top begins to appear, p53:DNA complex, with the addition of p53. This shows specific binding since Random 1 is not being a bound at the highest concentrations of p53. (b) Shows the binding curve, inner box, and scatchard plot, outer box, for recognition element *p21*. (c) Shows the binding curve, inner box, and scatchard plot, outer box, for the recognition element *PG*.

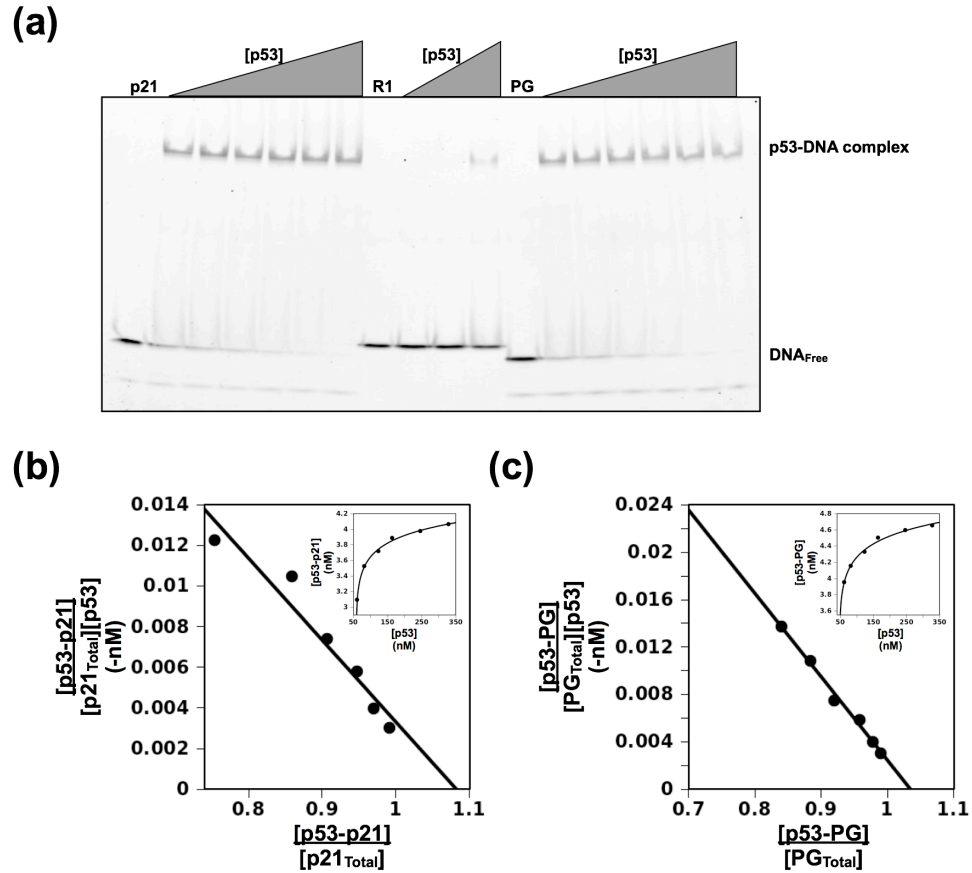


Figure 3.10. Binding Kinetics of Hyperstable p53-His for Recognition Sequences p21 and PG by EMSA. (a) Shows that EMSA done for Hp53-his. For both *p21* and *PG* the DNA_{free} band towards the bottom of the gel disappears, while a band towards the top begins to appear, p53:DNA complex, with the addition of p53. This shows specific binding since Random 1 is not being bound at the highest concentrations of p53. (b) Shows the binding curve, inner box, and scatchard plot, outer box, for recognition element *p21*. (c) Shows the binding curve, inner box, and scatchard plot, outer box, for the recognition element *PG*.

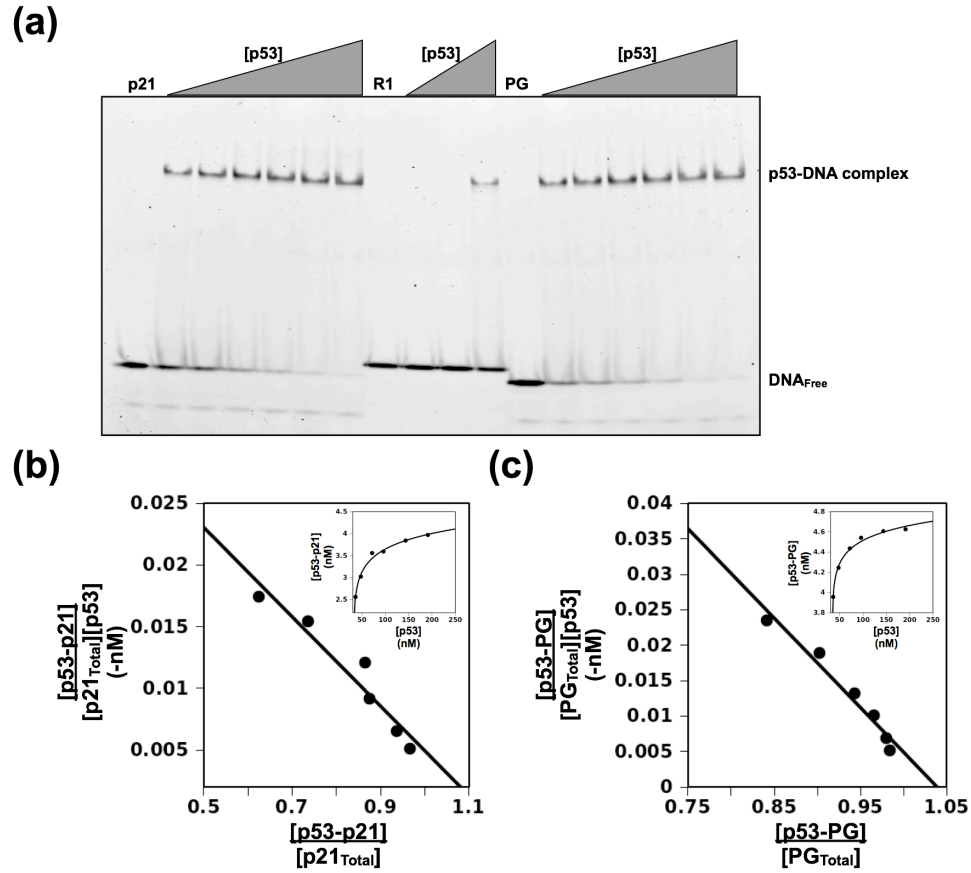


Figure 3.11. Binding Kinetics of Hyperstable p53 for Recognition Sequences p21 and PG by EMSA. (a) Shows that EMSA done for Hp53. For both *p21* and *PG* the DNA_{free} band towards the bottom of the gel disappears, while a band towards the top begins to appear, p53:DNA complex, with the addition of p53. This shows specific binding since Random 1 is not being a bound at the highest concentrations of p53. (b) Shows the binding curve, inner box, and scatchard plot, outer box, for recognition element *p21*. (c) Shows the binding curve, inner box, and scatchard plot, outer box, for the recognition element *PG*.

Table 3.1. Binding Kinetics Determined through EMSA for WTp53 and Hp53. Both the non-labeled DNA and thrombin controls were done using Hp53-His and only done once. All forms of p53; WTp53-His, Wtp53, Hp53-His, and Hp53 were done in triplicate.

	K_d (nM)	
	<i>p21</i>	<i>PG</i>
Non-labeled DNA control	57.500	37.482
Thrombin Control	39.918	19.014
WTp53-his	54.728 ± 50.739	35.341 ± 9.926
WTp53	70.845 ± 23.542	37.641 ± 19.760
Hp53-his	47.104 ± 24.613	14.782 ± 0.516
Hp53	23.027 ± 4.080	11.725 ± 3.782

The K_d 's for hyperstable p53 forms, Hp53-His and Hp53, were reasonable except for the K_d of Hp53-His for *p21*. It was 2-folds higher and had a larger deviation between its triplicates. The removal of the 6x-histidine tag from hyperstable p53 seemed to have a small affect on the binding energetics, about a 2-fold difference for *p21*. It also seemed that all the p53 forms, WTp53-His, WTp53, Hp53-His, and Hp53, had a higher affinity for *PG* over *p21* with 2-to-4 fold difference between the two.

CHAPTER IV

CONCLUSIONS

The p53 protein is a transcriptional factor that plays an important role in maintaining genomic stability through the process of transducing signals. The strong correlation between p53 function and cancer has led to substantial studies on p53 by many research groups. Due to the majority of p53 lacking tertiary structure, the full functionality of p53 is still unknown. To help close this gap, we propose to investigate domain-domain communication and how structural perturbations in one domain can effect the DBD ability to bind DNA. This will be done by mutational analysis of the binding energetics between p53 and different recognition sequences.

To move forward with the larger project above basic protocols were established. A recombinant system for synthesizing natively-folded p53 was developed using *E. coli*. By using *E. coli* as the expression system there will be no post-translational modifications made to p53, allowing for mutations to be the only changes in p53 when doing mutational analysis. To demonstrate that the oligomerization state of recombinant p53 is a tetramer similar to the physiological active species, a glutaraldehyde cross-linking protocol was developed. Lastly, the binding energetics of Wild Type p53 (WTp53) and Hyperstable p53 (Hp53) for *p21* and *PG* recognition elements were determined through EMSA.

In Chapter 3, it was shown that Recombinant human p53 was expressed and purified using *E. coli*, and the oligomeric state and energetics were determined. While the majority of hyperstable p53 was found to be in a tetrameric state, wild type p53 showed to have a significant presence of oligomeric aggregates, seen in the glutaraldehyde cross-linkings. This could possibly be due to the low yield of p53, ~ 400 nM, obtained during purification. In previous research the oligomerization constant between tetramers and dimers is between 50-250 nM⁶⁰⁻⁶¹ and when doing DNA binding assays the concentration of p53 used is within or below this amount. It has also been shown that aggergation will occur faster in wild type p53 than hyperstable p53 (M133L/V203A/N239Y/N258D).⁶⁰ Since wild type p53 was shown to exist in multiple oligomeric states the K_d 's found were not reliable. The K_d 's were also larger, at least 2-fold, than what's seen in other research, K_d for *p21* 4.3-5.5 nM⁵⁸ and for *PG* 14-18.1 nM⁵⁹. Which makes sense with the large presence of aggergates. To possibly eliminate the presence of oligomeric aggregates and increase tetramerzation within wild type p53, different solution conditions could be tested. It's been seen that the concentration of salt can affect p53:DNA binding ability and oligomerization.⁵³ The hyperstable p53 K_d 's determined were within reasonable proximity of what's been seen in previous research, K_d for *p21* 3-13 nM^{60, 62} (K_d for *PG* wasn't found). Both WT- and H-p53 seemed to have a higher energetic binding affinity for the recognition element *PG* over *p21*. This could be due to *PG* being a man made recognition element that was specifically designed for p53 binding.⁵²

With these results, we've shown we can express and purify recombinant p53, determine the oligomerization state, and calculate the binding energetics in our lab, which

was the main focus of this thesis. This will allow for our reasearch to move forward; into the larger project involving mutational analysis.

REFERENCES

1. Lane DP (1992) p53, guardian of the genome. *Nature* **358**, 15-16.
2. Levine AJ (1997) p53, the cellular gatekeeper for growth and division. *Cell* **88**, 323-331.
3. Bell S, Klein C, Müller L, Hansen S, Buchner J (2002) live or let die: cell's response to p53. *Nature Rev Cancer* **2**, 594-604.
4. Vogelstein B, Lane D, Levine AJ (2000) Surfing the p53 network. *Nature* **408**, 307-310.
5. Hollstein M, Rice K, Greenblatt M, Soussi T, Fuchs R, Sørli T, Hovig E, Smith- Sørensen B, Montesano R, Harris CC (1994) Database of p53 gene somatic mutations in human tumors and cells lines. *Nucl Acids Res* **22**, 3551-3555.
6. Hollstein M, Shomer B, Greenblatt M, Soussi T, Hovig E, Montesano R, Harris CC (1996) Somatic point mutations in the p53 gene of human tumors and cell lines: updated compilation. *Nucl Acids Res* **24**, 141-146.
7. Sharpless NE, DePinho RA (2007) Cancer biology: gone but not forgotten. *Nature* **445**, 606–607.
8. Ventura A, Kirsch DG, McLaughlin ME, Tuveson DA, Grimm J, Lintault L, Newman J, Reczek EE, Weissleder R, Jacks T (2007) Restoration of p53 function leads to tumour regression in vivo. *Nature* **445**, 661–665.
9. Xue W, Zender L, Miething C, Dickins RA, Hernando E, Krizhanovsky V, Cordon-Cardo C, Lowe SW (2007) Senescence and tumour clearance is triggered by p53 restoration in murine liver carcinomas. *Nature* **445**, 656-660.
10. Wright PE, Dyson HJ (1999) Intrinsically unstructured proteins: re-assessing the protein structure-function paradigm. *J Mol Biol* **293**, 321-331.

11. Uversky UN (2002) Natively unfolded proteins: a point where biology waits for physics. *Prot Sci* **11**, 739-756.
12. Dyson HJ, Wright PE (2005) Intrinsically unstructured proteins and their functions. *Nat Rev Mol Cell Biol* **6**, 197-208.
13. Dunker AK, Obradovic Z, Romero P, Garner EC, Brown CJ (2000) Intrinsic protein disorder in complete genomes. *Genome Inf Ser* **11**, 161-171.
14. Ward JJ, Sodhi JS, McGriffin LJ, Buxton BF, Jones DT (2004) Prediction and functional analysis of native disorder in proteins from the three kingdoms of life. *J Mol Biol* **337**, 635-645.
15. Oldfield CJ, Cheng Y, Cortese MS, Brown CJ, Uversky VN, Dunker AK (2005) Comparing and combining predictors of mostly disordered proteins. *Biochemistry* **44**, 1989-2000.
16. Perutz MF (1970) Stereochemistry of cooperative effects in haemoglobin. *Nature* **228**, 726-739.
17. Bray D, Duke T (2004) Conformational spread: the propagation of allosteric states in large multiprotein complexes. *Annu Rev Biophys Biomol Struct* **33**, 53-73.
18. Changeux JP, Edelstein SJ (2005) Allosteric mechanisms of signal transduction. *Science* **308**, 1424-1428.
19. Liu J, Perumal NB, Oldfield CJ, Su EW, Uversky VN, Dunker AK (2006) Intrinsic disorder in transcription factors. *Biochemistry* **45**, 6873-6888.
20. Bell S, Klein C, Müller L, Hansen S, Buchner J (2002) p53 contains large unstructured regions in its native state. *J Mol Biol* **322**, 917-927.
21. Dawson R, Müller L, Dehner A, Klein C, Kessler H, Buchner J (2003) The N-terminal domain of p53 is natively unfolded. *J Mol Biol* **332**, 1131-1141.
22. Wells M, Tidow H, Rutherford TJ, Markwick P, Jensen MR, Mylonas E, Svergun DI, Blackledge B, Fersht AR (2008) Structure of tumor suppressor p53 and its intrinsically disordered N-terminal transactivation domain. *Proc Natl Acad Sci USA* **105**, 5762-5767.
23. Tidow H, Melero R, Mylonas E, Freund SMV, Grossmann JG, Carazo JM, Svergun DI, Valle M, Fersht AR (2007) Quaternary structures of tumor suppressor p53 and a specific p53-DNA complex. *Proc Natl Acad Sci USA* **104**, 12324-12329.

24. Bochkareva E, Kaustov L, Ayed A, Yi GS, Lu Y, Pineda-Lucena A, Liao JCC, Okorokov AL, Milner J, Arrowsmith CH, Bochkarev A (2005) Single-stranded DNA mimicry in the p53 transactivation domain interaction with replication protein A. *Proc Natl Acad Sci USA* **102**, 15412-15417.
25. Kussie PH, Gorina S, Marechal V, Elenbaas B, Moreau J, Levine AJ, Pavletich NP (1996) Structure of the MDM2 oncoprotein bound to the p53 tumor suppressor transactivation domain. *Science* **274**, 948-953.
26. Hupp TR, Meek DW, Midgley CA, and Lane DP (1992) Regulation of the specific DNA binding function of p53. *Cell* **71**, 875-886.
27. Oda L, Arakawa H, Tanaka T, Matsuda K, Tanikawa C, Mori T, Nishimori H, Tamai K, Tokino T, Nakamura Y, and Taya Y (2000) p53AIP1 a potential mediator of p53-dependent apoptosis, and its regulation by Ser-46-phosphorylated p53. *Cell* **102**, 849-862.
28. Keller DM, Zeng X, Wang Y, Zhang QH, Kapoor M, Shu H, Goodman R, Lozano G, Zhao Y, Lu H (2001) A DNA damage-induced p53 serine 392 kinase complex contains CK2, hSpt16, and SSRP1. *Mol Cell* **7**, 283-292.
29. Walker KK, Levine AJ (1996) Identification of a novel p53 functional domain that is necessary for efficient growth suppression. *Proc Natl Acad Sci USA* **93**, 15335-15340.
30. Yu H, Chen JK, Feng S, Dalgarno DC, Brauer AW, Schrelber SL (1994) Structural basis for the binding of proline-rich peptides to SH3 domains. *Cell* **76**, 933-945.
31. Arnott S, Dover SD (1968) The structure of poly-L-proline II. *Acta Crystallogr B* **24**, 599-601.
32. Sasisekharan V (1959) Structure of poly-L-proline II. *Acta Cryst* **12**, 897-903.
33. Wang P, Reed M, Wang Y, Mayr G, Stenger JE, Anderson ME, Schwedes JF, Tegtmeyer P (1994) p53 domains: structure, oligomerization, and transformation. *Mol Cell Biol* **14**, 5182-5191.
34. Sakamuro D, Sabbatini P, White E, Prendergast GC (1997) The proyl-proline region of p53 is required to activate apoptosis but not growth arrest. *Oncogene* **15**, 887-898.

35. Müller-Tiemann BF, Halazonetis TD, Elting JJ (1997) Identification of an additional negative regulatory region for p53 sequence-specific DNA binding. *Proc Natl Acad Sci USA* **95**, 6079-6084.
36. Zheng H, You H, Zhou XZ, Murray SA, Uchida T, Wulf G, Tang X, Lu KP, and Xiao ZX (2002) The prolyl isomerase Pin1 is a regulator of p53 is genotoxic response. *Nature* **419**, 849-853.
37. Hupp TR, Sparks A, Lane DP (1995) Small peptides activate the latent sequence-specific DNA binding function of p53. *Cell* **83**, 237-245.
38. Nakamura S, Roth JA, Mukhopadhyay T (2000) Multiple lysine mutations in the C-terminal domain of p53 interfere with MDM2-dependent protein degradation and ubiquitination. *Mol Cell Biol* **24**, 9391-9398.
39. Gu W, and Roeder RG (1997) Activation of p53 sequence-specific DNA binding by acetylation of the p53 C-terminal domain. *Cell* **90**, 595–606.
40. Nikolova PV, Henckel J, Lane DP, Fersht AR (1998) Semirational design of active tumor suppressor p53 DNA binding domain with enhanced stability. *Proc Natl Acad Sci USA* **95**, 14675-14680.
41. Welch M, Govindarajan S, Ness JE, Villalobos A, Gurney A, Minshull J, Gustafsson C (2009) Design parameters to control synthetic gene expression in *Escherichia coli*. *PLoS One* **4**, e7002.
42. Gentz R, Bujard H (1985) Promoters recognized by *Escherichia coli* RNA polymerase selected by function: highly efficient promoters from bacteriophage T5. *J. Bacteriol* **164**, 70-77.
43. Shapiro AL, Vinuela E, Maizel Jr. JV (1967) Molecular weight estimation of polypeptide chains by electrophoresis in SDS-polyacrylamide gels. *Biochemical and Biophysical Research Communications* **28**, 815-820.
44. Meyer TS, Lamberts BL (1965) Use of coomassie brilliant blue R250 for the electrophoresis of microgram quantities of parotid saliva proteins on acrylamide-gel strips. *Biochem Biophys Acta* **107**, 144-145.
45. Whitten ST, Garcis-Moreno BE (2000) pH dependence of stability of staphylococcal nuclease: evidence of substantial electrostatic interactions in the denatured state. *Biochemistry* **39**, 14292-14304.

46. Simonian MH (2002) Spectrophotometric determination of protein concentration. *Current Protocols in Cell Biology*. A.3B.1-A.3B.7.
47. Bradford M (1976) A rapid and sensitive method for the quantitation of microgram quantities of protein utilizing the principle of protein-dye binding. *Anal Biochem* **72**, 248-254.
48. Towbin H, Staehelin T, Gordon J (1979) Electrophoretic transfer of proteins from polyacrylamide gels to nitrocellulose sheets: procedure and some applications. *Proc Natl Acad Sci USA* **76**, 4350-4354.
49. Bonsing BA, Corver WE, Gorsira MC, van Vliet M, Oud PS, Cornelisse CJ, Fleuren GJ (1997) Specificity of seven monoclonal antibodies against p53 evaluated with Western blotting, immunohistochemistry, confocal laser scanning microscopy, and flow cytometry. *Cytometry* **28**, 11-24.
50. Stenger JE, Mayr GA, Mann K, Tegtmeyer P (1992) Formation of stable p53 homotetramers and multiples of tetramers. *Mol Carcinog* **5**, 102-106.
51. Migneault I, Dartiguenave C, Bertrand MJ, Waldron KC (2004) Glutaraldehyde: behavior in aqueous solution, reaction with proteins, and application to enzyme crosslinking. *BioTechniques* **37**, 790-802.
52. el-Deiry WS, Kern SE, Pietenpol JA, Kinzler KW, Vogelstein B (1992) Definition of a consensus binding site for p53. *Nature Genet* **1**, 45-49.
53. Weinberg RL, Veprintsev DB, Fersht AR (2004) Cooperative binding of tetrameric p53 to DNA. *J Mol Biol* **341**, 1145-1159.
54. Kibbe WA (2007) OligoCalc: an online oligonucleotide properties calculator. *Nucleic Acids Res* **35**, W43-W46.
55. Hellman LM, Fried MG (2007) Electrophoretic mobility shift assay (EMSA) for detecting protein-nucleic acid interactions. *Nature Protocols* **2**, 1849-1861.
56. Maio F, Bouziane M, O'Connor TR (1998) Interaction of the recombinant human methylpurine-DNA glycosylase (MPG protein) with oligodeoxyribonucleotides containing either hypoxanthine or abasic sites. *Nucl Acids Res* **26**, 4034-4041.
57. Kishore AH, Batta K, Chandrima D, Agarwal S, Kundu TK (2007) p53 regulates its own activator: transcriptional co-activator PC4, a new p53-responsive gene. *Biochem J* **406**, 437-444.
58. Weinberg RL, Veprintsev DB, Bycroft M, Fersht AR (2005) Comparative binding of p53 to its promoter and DNA recognition elements. *J Mol Biol* **348**, 589-596.

59. Wölcke J, Reimann M, Klumpp M, Göhler T, Kim E, Deppert W (2003) Analysis of p53 “latency” and “activation” by fluorescence correlation spectroscopy. *J Biol Chem* **278**, 32587–32595.
60. Rajagopalan S, Huang F, Fersht AR (2010) Single-molecule characterization of oligomerization kinetics and equilibria of the tumor suppressor p53. *Nucl Acids Res* **39**, 2294-2303.
61. Veprintsev DB, Freund SMV, Andreeva A, Rutledge SE, Tidow H, Cañadillas JMP, Blair CM, Fersht AR (2005) Core domain interactions in full-length p53 in solution. *Proc Natl Acad Sci USA* **103**, 2115–2119.
62. Natana E, Hirschberg D, Morgner N, Robinson CV, Fersht AR (2009) Ultraslow oligomerization equilibria of p53 and its implications. *Proc Natl Acad Sci USA* **106**, 14327–14332.

VITA

Leasha Janece Schaub was born in Lubbock, Texas, on March 23, 1988, the daughter of Janice Jolene Schaub and Lowry Paul Schaub. After completing her work at Monterey High School, Lubbock, Texas, in 2006, she entered Texas State University-San Marcos. During the Summer of 2007, she attended South Plains College in Plainview, Texas. She received the degree of Bachelor of Science in Biochemistry from Texas State in May 2010. During the following years she was employed as an Instructional Assistant for General Chemistry I and Biochemistry laboratories at Texas State. In August 2010, she entered the Graduate College of Texas State.

Permanent Address: leashaschaub@yahoo.com

This thesis was typed by Leasha J. Schaub.